Marine Geology
June 2024, Volume 472, Pages 107292 (16p.)
https://doi.org/10.1016/j.margeo.2024.107292 https://archimer.ifremer.fr/doc/00889/100054/

Suspended particulate matter response to extreme forcings in the Bay of Seine

Poppeschi Coline [1], Verney Romaric [2,*], Charria Guillaume [1]

[1] Ifremer, Univ. Brest, CNRS, IRD, Laboratory for Ocean Physics and Satellite remote sensing (LOPS), IUEM, 29280 Brest, France
[2] Ifremer, DYNECO, Hydrosedimentary Dynamics Laboratory (DHYSED), 29280 Brest, France

* Corresponding author : Romaric Verney, email address : romaric.verney@ifremer.fr

Abstract :

The latest Intergovernmental Panel on Climate Change report of 2023 alerts about an increase in the occurrence and intensity of extreme hydro-meteorological events such as storms and extreme river flows, i.e. drought and floods. Investigating the occurrence of these extreme events in the past 15 years and their impacts on sediment dynamics will provide crucial knowledge for anticipating future trajectories of coastal ecosystems. Time series from in situ observations are analyzed to identify extreme events of river flows and waves and examine their impact on Suspended Particulate Matter (SPM) dynamics in a highly turbid coastal area equipped with a high frequency in situ monitoring station at the interface between the Seine Estuary and the Bay of Seine (northern coast of France). Extreme river flow and wave orbital velocity events are investigated because high river discharge contributes to deliver large amounts of SPM concentration to the bay and strong wave action within the bay can lead to erosion and resuspension of bottom sediments. An original detection method is proposed, based on high frequency in situ observations combined with satellite and model data from 2006 to 2022. Extreme forcings are examined through their specific characteristics (high intensity, long duration, season of occurrence, succession of events), their impact on SPM concentration in the coastal environment and the comparison to mean seasonal dynamics. A positive relationship exists between SPM concentration and high SPM spatial extent and forcing intensity. Extremes are more intense in winter for both forcings and generate larger SPM concentration anomalies. However, extreme events during late spring/summer, periods or mean low forcing intensity, are demonstrated to generate SPM concentration anomalies up to 4 times larger than the monthly mean value, hence possibly strongly impacting the system during these atypical periods. This is particularly important as analyzing the distribution of extreme river flow events over the last 60 years indicated an increase in their occurrence and more important the progressive occurrence of high intensity extreme events during spring/summer periods.

Highlights

► Time dependent climatologies are used to identify and characterize extreme events from forcings and SPM concentration anomaly. ► Extreme event impact is seasonally variable, but relatively as much important in summer as in winter. ► Extreme river flow event become more frequent over the last 60years and their seasonality changed, with more events in spring over the last decades.

Keywords : Suspended particulate matter, Surface waves, River flows, Extreme events, Coastal ocean.

1. Introduction

Global change is increasing extreme event occurrence and intensity in the ocean (IPCC, 2021 & 2023) such as marine heatwaves and cold spells (Simon et al., 2023) or storms and river flows (Garner et al., 2015; Poppeschi et al., 2021) observed for example in the Bay of Biscay and the English Channel. Extreme events are characterized by atypical high or low intensity values, compared to a threshold. This threshold is often determined from statistical analysis and can be fixed or time-varying depending on the target question. Although some extremes such as marine heatwaves and their effects on coastal ecosystems are increasingly explored (Izquierdo et al., 2022; Simon et al., 2023), others are less documented, such as extreme wave

and river flow events and their impact on Suspended Particulate Matter (SPM) concentration in the land-sea interface.

However, sediment transport is a key process in estuarine and coastal ecosystem dynamics. Rivers transport particles (and associated contaminants) which can be exported to adjacent seas (Gangloff et al., 2017) or settle in low energy areas in estuarine and coastal environments such as mudflats (Deloffre et al., 2006, Cheng et al., 2013) or river deltas (Dufois et al., 2014). Estuaries are particular environments accumulating sediments in turbidity maximum areas (Le Hir et al., 2001; Burchard et al., 2018; Grasso et al., 2018), that can be flushed out toward the estuary mouth or adjacent bays during high river flow periods. Storms induce large bed shear stress, larger than tidal-induced shear stress, erode bed sediments and yield to high SPM concentration and control sediment fluxes in coastal areas and estuary mouths (Fettweis et al., 2010; Nowacki and Ganju, 2018; Tang et al., 2019; Schulz et al., 2018; Verney et al., 2024). Consequently, SPM dynamics affect physical habitat characteristics in estuaries and coastal seas, and also drive their morphology at longer time scales (Grasso et al., 2021). Cascading effects are also observed along the ecosystem, impacting primary production (Cloern et al., 1987; Schallenberg and Burns, 2004; Poppeschi et al., 2022); water quality (Cailleaud et al., 2007; Chen et al., 2019); and fish foraging behavior (Figueiredo et al., 2019).

Rare are the studies that examine specific events (e.g. storms, floods), which can be intense but not necessarily exceptional, or “extreme”. Even rarer are those who examine the occurrence of extreme meteorological or hydrological events on estuaries and coastal seas and their consequences on sediment dynamics (Lettmann et al., 2009; Tavora et al., 2023; Fan et al., 2023), and most of them focus on a single extreme event. Hence, most observations and conclusions are event-based, and cannot be generalized to offer broader perspectives.

Extreme events are often short, intense, rare and stochastically distributed (McPhillips et al., 2018), which make them difficult to be captured by weekly monitoring programs. The motivation of this study consists in the implementation of an original methodological approach to detect extreme river flow and wave events and examine the SPM dynamic through multiple available data sets: *in situ*, model and satellite data. Here, we investigate the response of SPM concentration (hereafter SPMC) to extreme events over 16 years (2006 - 2022) at the interface between the Seine estuary and its adjacent bay to understand how extreme event characteristics (intensity, duration, seasonality, succession of events) impact the SPM dynamics. Even if the considered time series appear to be short, they can be used to analyze in detail the variability of extreme events. Schlegel et al. (2019) for marine heatwaves mentioned that 10 years of data can be enough to have the same similarities of extreme events than the usual 30 years of data. A comparison is also made between the impact of extreme events and the impact of mean seasonal forcings on SPM dynamics.

2. Data and methods

2.1 Description of the eastern part of the Bay of Seine

The Bay of Seine is located at the interface between the estuary of the Seine River and the eastern part of the Bay of Seine, which is connected to the English Channel (Figure 1). It is a shallow bay with a maximum depth of 30m and has an area of approximately 4000km^2 (Aminot *et al*., 1997). The Bay of Seine is a semi-diurnal macrotidal environment (tidal range up to 7m at Le Havre) with average tidal currents of 0.5 to 1m s^{-1} (Salomon and Breton, 1991) during spring tides. The Bay of Seine is connected to the Seine estuary, one of the largest

northwestern European estuaries, and driven by the Seine River with a flow rate between 100 and 2300m^3 s^{-1} (Schulz *et al.*, 2018). Tides in the Bay of Seine play an important role in sediment distribution by depositing mud from the shallow subtidal zone to the open estuary and distributing sand, especially from the sandbanks at the mouth of the estuary (Lesourd *et al.*, 2003). The Seine estuary has an Estuarine Turbidity Maximum (ETM) located 10km upstream of the mouth around Fatouville during normal river flow (Figure 1). During periods of high river flow this ETM is flushed out to the mouth and during low river flow conditions it can move upstream within the estuary (Grasso et al., 2018). The average cumulative sediment supply from the Seine River is 725 10^3tons per year (Grasso *et al.*, 2018; Schulz *et al.*, 2018) and mainly during high river flow (Landemaine, 2016). The prevailing winds come from the west-southwest with speeds that can exceed 8m s^{-1}. Surface waves mainly enter the bay from the northwest (Schulz *et al.*, 2018) with a wave orbital velocity that can exceed 0.7m s^{-1}.

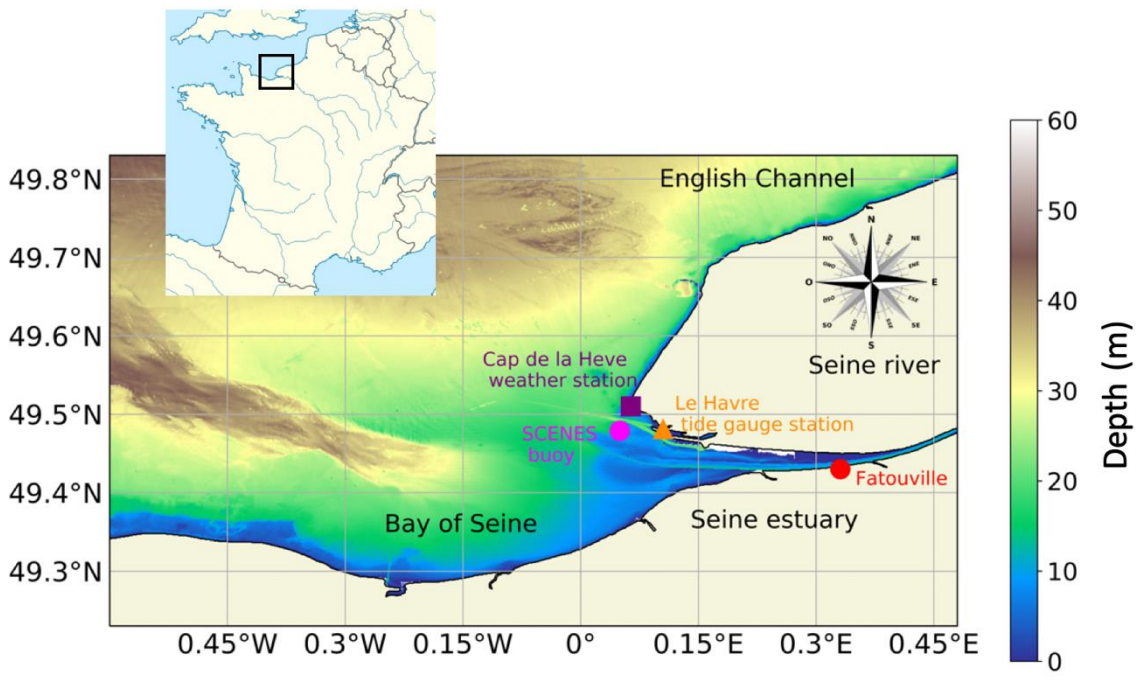

Figure 1: Bathymetry of the Bay of Seine. The pink circle indicates the COAST-HF Scenes buoy, the orange triangle “Le Havre” tide gauge station, the purple square the “Cap de la Hève” weather station and the red circle the ETM location at Fatouville.

2.2 Datasets

2.2.1 Forcings data

Daily river flows are measured at the Vernon gauging station located 200 km upstream of the mouth, outside of the estuary tidal limit (1.477°E, 49.083°N - French hydrology database: www.hydro.eaufrance.fr). We consider that the propagation time of the river flow to the mouth is on average 5 days (Artelia, 2019). Over the considered period, from 2006 to 2022, river flows vary from 40 to 2280m^3 s^{-1} with a maximum in late winter. Wind direction and intensity are retrieved every hour from the meteorological station *Cap de la Hève* (Figure 1) from Météo-France observation network (https://donneespubliques.meteofrance.fr).

Significant wave height (Hs) is often used to represent wave forcing. However, we have chosen to consider the square of wave orbital velocity as a representative metric of wave forcing because it is a better proxy for erosion processes (Soulsby *et al*., 1993). Hourly wave orbital velocity data are available from WaveWatch3 model simulations (Rolland and Ardhuin, 2014) through the MARC web portal (marc.ifremer.fr) and extracted at the nearest grid point of the SCENES buoy.

Sea levels are provided at high and low tides by the Shom (http://data.shom.fr) at Le Havre tide gauge station (Figure 1).

2.2.2 *In situ* SPMC data measured at the SCENES buoy

This study is based on high-frequency data measured by a moored coastal buoy called SCENES, part of the French national observation network COAST-HF (Répécaud *et al*., 2019; Farcy *et al*., 2019; Cocquempot *et al*., 2019) from the French national Research Infrastructure ILICO (https://www.ir-ilico.fr/). SCENES has been deployed at the Seine estuary mouth since 2015 at 15m depth (Figure 1). The SCENES buoy monitors SPMC every 15min at the surface (-2m below surface) and 30min at the bottom (+0.5m above bottom) using Wetlabs optical turbidimeters. This dataset is fully described in Verney et al. (2024) and briefly reminded hereafter. The optical measurements were converted to SPMC (g L^{-1}) using *in situ* water samples. Before October 2017, SPM measurements were taken +1.5m over the bottom. After this date, a Nortek AWAC Acoustic Doppler Current Profiler (ADCP) together with optical measurements were used to evaluate SPMC at the bottom 1.5m above the bed. To analyze the influence of wave and flow forcings, and because the tide contributes significantly to the variability of the SPMC signal, SPMC anomalies are used. These anomalies correspond to the difference between the raw signal and the mean intratidal high frequency signal (by tidal range classes) for low wave activity (Hs<1m) and mean river discharge (Q=[300 500]m^3 s^{-1}) conditions. Anomalies hence correspond to the SPMC high frequency signal filtered from the tidal-induced influence (Refer to Verney et al., 2024, for detailed information). Raw SPMC anomalies are reduced to tidal-percentile values (P50 and P90) to provide characteristic metrics at the tidal scale.

2.2.3 Results of the hydro-sedimentary hindcast model (ARES archive)

The 3D "CurviSeine" model provides hourly SPMC in g L^{-1} in the Seine estuary and its bay (ARES project, Grasso *et al*., 2020; 2021) from 2006 to 2019. The model has 10 sigma levels and a spatial resolution ranging from 4km offshore to 100m in the Seine estuary. This

model configuration couples a curvilinear primitive equation hydrodynamic model (MARS3D, Lazure and Dumas, 2008) and a hydro-sedimentary model that takes into account advection, erosion, deposition and consolidation processes of different sand/mud sediment classes (MUSTANG, Le Hir *et al.*, 2011; Grasso *et al.*, 2015; Mengual et al., 2017), and is coupled with a spectral wave model (WW3, Rolland and Ardhuin, 2014).

Model open boundary conditions are set hourly and derived i) for wave inputs from a WW3 regional model at 10 km resolution, ii) for temperature, salinity and tides from a regional (shelf-scale) MARS3D configuration at 2.5km resolution (https://marc.ifremer.fr/, Grasso *et al.*, 2018) and for atmospheric forcings from the Météo-France AROME atmospheric model at 1.3km resolution (https://donneespubliques.meteofrance.fr). The temperature, salinity and SPMC outputs from the model have been compared and validated with the PHRESQUES measurement network (Grasso *et al.*, 2020 - ARES report). Model data are considered for the second vertical level from the bottom (k=2). We use validated model data in addition to observation (Figure S1) to assess the overall behavior of the events for all years and seasons. SPMC data from the model show a similar qualitative dynamic behavior as observations, while overestimated compared to the buoy data (Figure S1). Similarly to *in situ* observations, modelled SPMC data are represented by anomalies and reduced to percentile values (P50 and P90) at the tidal scale.

2.2.4 Satellite data

L4 images from the SeaWiFS, MODIS and MERIS instruments are processed with the OC5 algorithm (Gohin, 2011) to explore the spatial extent of the surface sediment plume in the Bay of Seine. Daily data are available from January 1^{rst} 2006 to December 16th 2022 with a 1.1km spatial resolution. L4 satellite data are compared with *in situ* data (Figure S2) and used to

observe the impact of extreme events on the spatial extent of surface SPMC. Data are available on https://marc.ifremer.fr/en and are processed by the Satellite Data Processing and Distribution Center (CERSAT) at Ifremer.

2.3 Data processing

2.3.1 Detection and characterization of extreme events

The Peak Over Threshold (POT) method is used to detect extreme wave and river flow events from 2006 to 2022 (Figure 2). Daily river flow data are interpolated at each high tide (semi-diurnal cycle, i.e. ~2 per day). The percentile 90 of hourly square wave orbital velocity is used to characterize wave conditions at each tidal cycle. These tidal percentiles 90 are aggregated by successive tides from January 1 to December 31 to create an annual climatology over the 2006-2021 period (2021 is the last full year of forcing time series) (Figure 2). This climatology computed at each tidal cycle is smoothed on a 30-day rolling window still calculating the percentile 90 to obtain a dynamic threshold. Extreme wave events correspond to wave orbital velocities exceeding the tidal percentile 90 smoothed threshold.

The same method is applied to detect extreme river flow events, but in order to additionally detect start and end dates of these events properly the percentile 75 is used. Thus, events are fully detected and not only short isolated peaks in river flow time series.

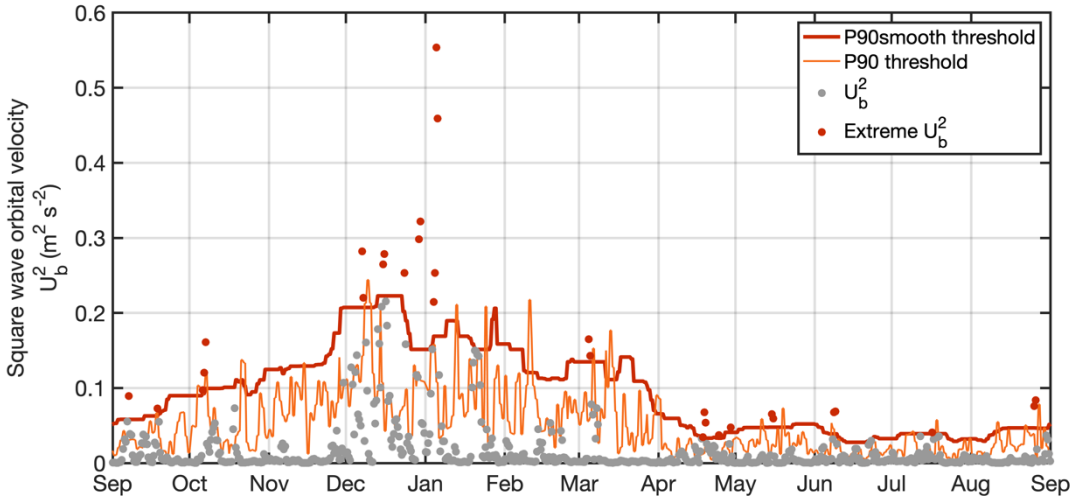

Figure 2 : Scheme of the extreme detection method with the example of wave forcing for the year 2011-2012. Tidal-P90 square wave orbital velocity (U_b^2) are represented by grey dots and extreme values by red dots. The annual climatology computed with the percentile 90 is shown by the orange line. The threshold (red thick line) corresponds to the smoothing of the percentile 90 of the orange line over one month moving period. Values above this threshold (red thick line) are therefore identified as extreme and are represented by red dots.

Four key parameters have been considered to characterize extreme events: intensity, intensity above threshold, duration and succession of events (Stephenson, 2008; Figure 3). A succession of events is detected when there are less than a week between two consecutive events (between the end of one event and the start of the next event). The concomitance of extreme river flow and wave forcings is studied to observe the response of SPMC during cumulated forcings.

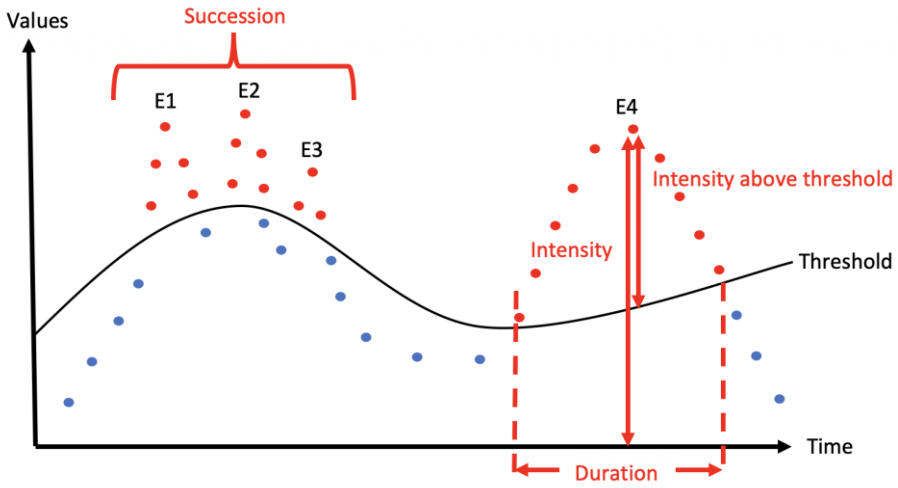

Figure 3 : The succession of extreme events, their intensities, their intensities above the threshold and their durations are illustrated on this scheme: extreme events with extreme values in red points, non-extreme values in blue points and the threshold in black line. In this example there are 4 extreme events detected: E1, E2, E3 and E4.

2.3.2 Spatial extent of SPMC events

A subset of L4 satellite data is used at the estuary/bay interface (0.3°W;0.3°E and 49.3°N; 49.7°N) to study SPMC spatial variability in the bay of Seine. Following Gangloff et al. (2017), a characteristic SPMC threshold is used to delineate the surface SPMC plume against the average background SPMC observed in the Eastern Bay of Seine. For our study area, a surface SPMC threshold value of 5mg L^{-1} was calculated from the mean SPMC distribution from all available images during the study period (2006 - 2022).

3. Results

3.1 Extreme events

Extreme wave and river discharge events are first identified from the long-term time series and analyzed further (Figure 4). 20 extreme river flow events are detected: from 0 to 2 events per year (average of 1.25 per year), none in 2009 and 2019. 211 extreme wave events were detected during the same period: from 5 to 22 events per year (average of 13 per year), 5 in 2010 and 22 in 2007.

Using a time-varying threshold over the annual cycle enables detection of extreme events over all seasons, i.e. not only extremely high river flows in winter, but also moderate river flow events during summer, a period of low mean river flow. Extreme river flow events show a marked seasonality with moderate intensity events in summer ($<800 m^3 s^{-1}$) versus intense floods in winter and spring reaching values above $1100 m^3 s^{-1}$ (Figure 5). In general, the stronger the river discharge event, the longer the event: summer events last from 4 to 90 tides, while winter event duration ranges from 18 to more than 100 tides. Short (<50tides) but high ($Q>1000 m^3 s^{-1}$) extreme river discharge events are also observed. An exceptional intense extreme event was observed in June 2016, reaching $2000 m^3 s^{-1}$ while the average river discharge for this period is lower than $400 m^3 s^{-1}$.

Extreme wave events are almost rare in April and June (13 and 12 events over the full period) and most frequent in winter (up to 20 events per month) (not shown). Similarly to extreme river flow events, extreme wave event intensity shows a significant seasonal variability, with strong peaks of maximum square wave orbital speed per event in winter (maximum $>0.4 m^2 s^{-2}$, average $0.24 m^2 s^{-2}$) and weaker values in summer (minimum $<0.2 m^2 s^{-2}$, average $0.07 m^2 s^{-2}$; Figure 5). Most of the extreme wave events detected are short and last on average 2 tides per event, whatever the season, and the longest reach 7 tides.

Several event successions are observed over the study period (Figure 4). The extreme forcing event successions are characterized most of the time by a group of 2 events only. No high intensity river flow successive ($Q>1000m^3\ s^{-1}$) were detected, but four were reported, separated by 2 weeks (April 2008; January 2011; May 2013 and January-February 2018). 66 wave event successions are detected. November to March is the most favorable season for successive wave events with 41 successive events detected (from 2006 to 2022). An exceptional succession of wave event was reported between February 10th 2020 and February 26th 2020, with 5 successive events.

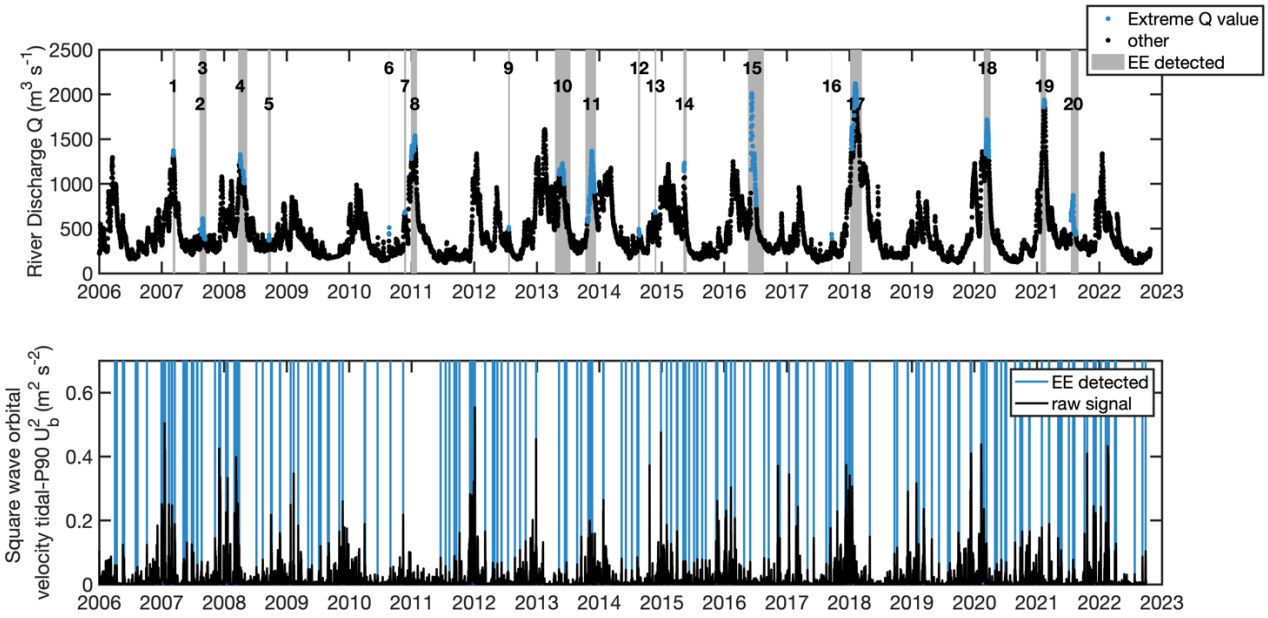

Figure 4 : Extreme forcing events from river flow (extreme values in blue points, extended extreme period in grey on top figure) and square wave orbital velocity (blue lines on bottom figure).

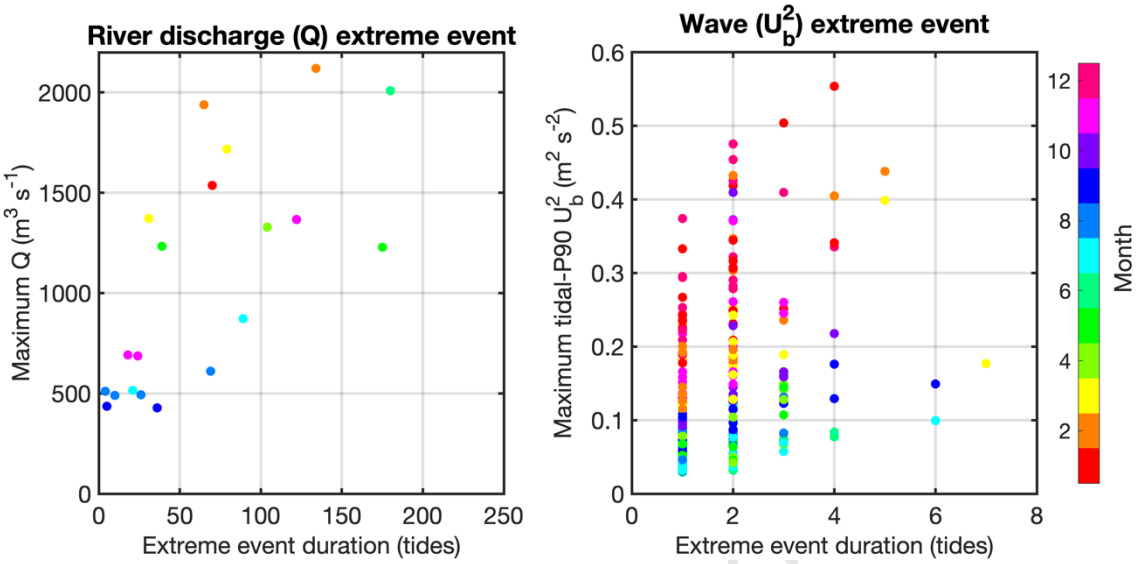

Figure 5 : Characterization of extreme forcing events of river flow (left) and square wave orbital velocity (right) through their duration, their intensity and the month of occurrence.

3.2 Suspended Particulate Matter Concentration (SPMC) anomalies in response to extreme events

3.2.1 SPMC anomaly time series

In situ and modelled SPMC anomalies present a high seasonal and interannual variability (Figure 6). Observed SPMC anomalies are globally higher at the bottom (values generally between -0.01 and 0.2gL^{-1}) than at the surface (values between -0.01 and 0.05g L^{-1}). Both surface and bottom anomalies are high and positive during winter and low or negative during summer. They present a similar interannual variability, with lower surface and bottom anomalies during winter 2016-2017 while the highest winter values are observed in 2017-2018 and 2021-2022.

The dynamics of *in situ* and model SPMC anomalies show similar seasonal patterns, while model SPMC anomalies are globally larger than the observed anomalies.

An extreme river flow or wave event is generally associated with a peak in SPMC anomaly, but not necessarily to an extreme anomaly value (Figure 6). Hence, extreme events do not explain all the sediment variability observed at the river mouth.

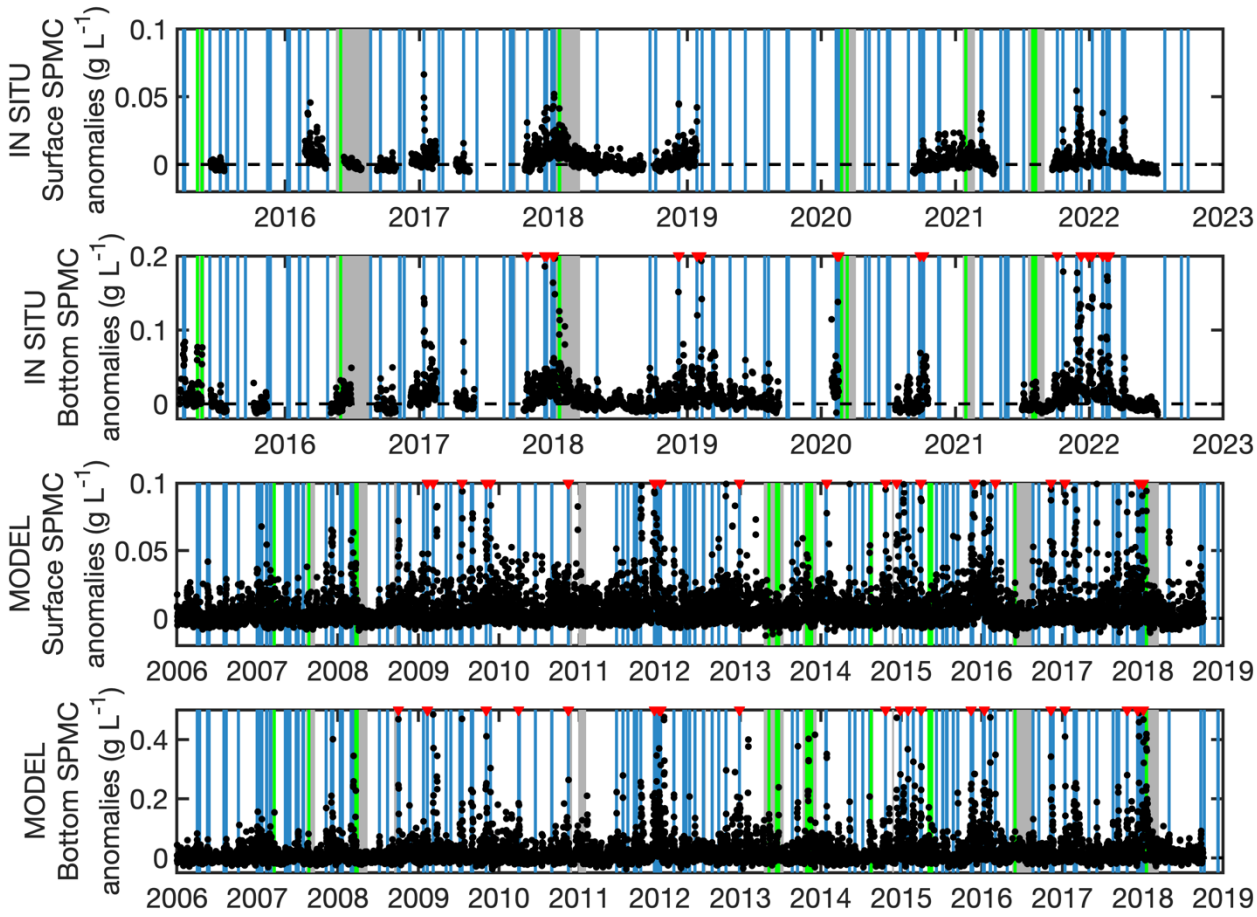

Figure 6 : Tidal-P50 SPMC anomalies observed with *in situ* data (a – surface, b- bottom) and model data (c – surface, d - bottom) during extreme river flow events (grey), extreme wave events (blue) and concomitant events (green). Red triangles artificially represent high values above 0.2g L^{-1} (*in situ* bottom), 0.1g L^{-1} (model surface) and 0.5g L^{-1} (model bottom).

Hereafter in section 3.2, in order to characterize SPMC anomalies during extreme events, the average anomaly value over the event period is calculated, both for extreme wave or river flow events.

3.2.2 Relation between extreme forcings and SPMC anomalies

SPMC anomalies related to wave extreme events can often exceed those related to river flow events; at the surface values are less or around 0.02g L^{-1} for river flow events versus 0.05g L^{-1} for wave events. At the bottom SPMC anomalies during river flow events do not exceed 0.1g L^{-1} for *in situ* and model data while they can exceed 0.5g L^{-1} for *in situ* and model data for waves events (not shown).

A positive trend can be observed between wave extreme events intensity and SPM response (Figure 7): the more intense the forcing, the stronger the SPMC anomaly. This is both observed in model and *in situ* data. Seasonality is observed with SPMC anomaly values close to 0 in summer and with the highest SPMC anomalies occurring in winter. Stronger events are detected with values larger than 0.025 and 0.1g L^{-1} for *in situ* data at the surface and the bottom respectively. The same patterns are observed with model data, with a 2-fold increase in SPMC anomaly values.

These seasonal differences can be explained by the erosion processes driving resuspension events. Sediment erosion fluxes are governed by an excess bed shear stress and an erosion rate. This excess bed shear stress is the difference between wave-current bed shear stress and the critical erosion shear stress, a threshold that expresses the resistance of the bed to erosion. Hence, in general, the larger the orbital velocity, the larger the bed shear stress and the eroded sediment flux. In winter, a high wave intensity season, extreme events detected are characterized by high wave orbital velocity values, and hence high excess shear stress and high SPMC anomalies. In summer, wave extreme events are generally weaker, and then both the excess shear stress, the erosion flux and SPMC anomalies are weaker.

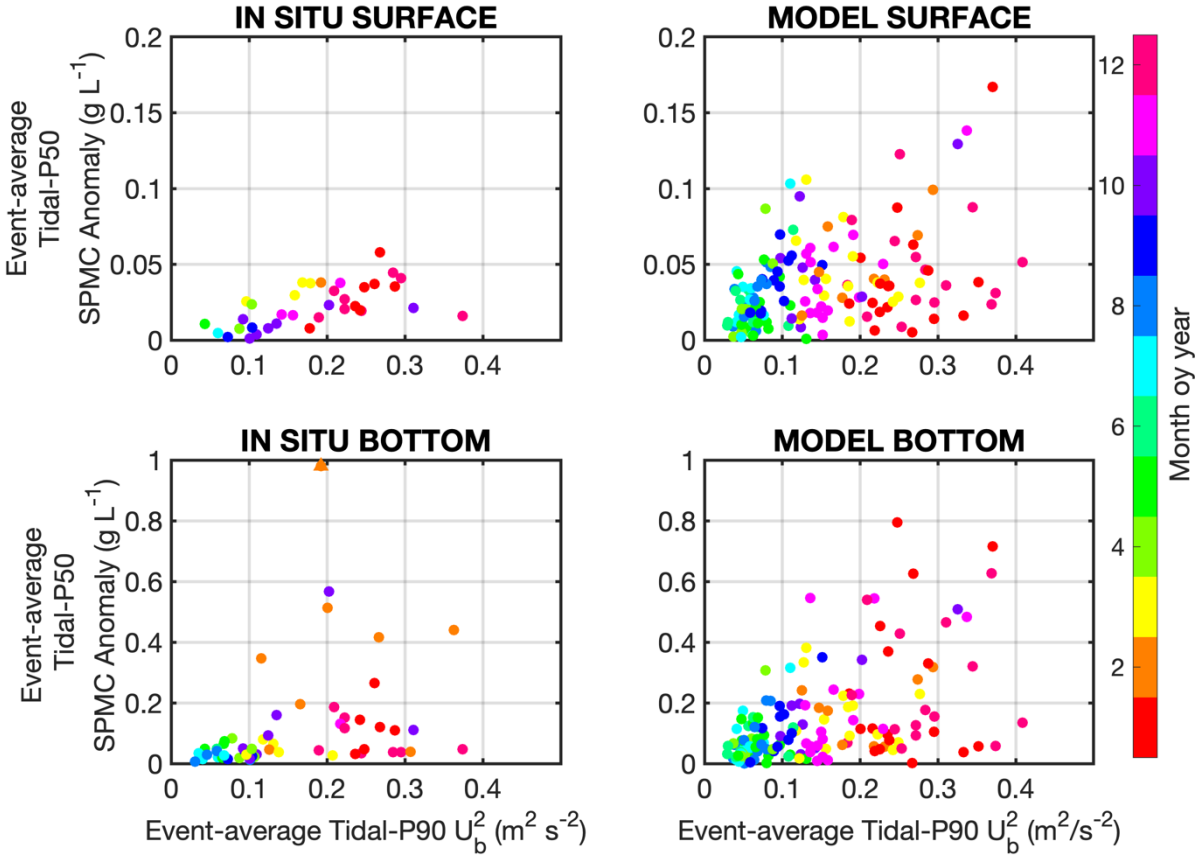

Figure 7 : Relation between event-average square wave orbital velocity and event-average Tidal-P50 SPMC anomalies during extreme wave events. The colors represent the months of the year. *In situ* data (2015-2022) are on the left and model data (2006-2019) are on the right. Surface data are on top panels and bottom data on bottom panels. The orange triangle artificially indicates the presence of an extremely high bottom SPMC anomaly (1.3g L^{-1}) observed in *in situ* data.

Investigating the influence of extreme river flow events is more complex as nearly all extreme river flow events are concomitant with several (or many) extreme wave events (Figure 6).

3.2.3 Impact of successive extreme wave events on the intensity of SPMC and their anomalies

In mixed sand/mud environments, such as the Seine estuary mouth, the concentration of fine sediment in suspension is strongly driven by the availability of fine sediments in the

surface layer of the bed. We questioned here if a succession of extreme wave events could i) wash out fine sediment from the surface layer, and hence decrease SPMC anomaly, event after event or ii) progressively destabilize bed sediments and hence increase their erodibility and finally increase SPMC anomaly. However, analyzing the SPMC anomaly dynamics of successive wave events did not show any strong trends that may support any of these two hypotheses. In particular, no *in situ* data are available during the periods with more than 4 successive events. But our investigations highlighted that the time lag between successive events controls the capacity for the system to return to an undisturbed tidal-driven situation. The following SPMC index is used to evaluate this time-lag effect:

$$[SPMC]\ index_{i,i+1} = \frac{\frac{[SPMC]_{max,i} + [SPMC]_{max,i+1}}{2} - \min([SPMC]_{i,i+1})}{\frac{[SPMC]_{max,i} + [SPMC]_{max,i+1}}{2}}$$

Where $[SPMC]_{max,i}$ represents the maximum SPMC of the event i (from the raw high frequency SPM concentration time series) and $[SPMC]_{i,i+1}$ represent raw (high frequency) SPMC between two successive event maxima i and i+1.

A low value of the [SPMC]index indicates that the SPMC between 2 consecutive events remains high, i.e. SPM settling velocity is lower or turbulent mixing remains high enough to counterpart settling (Figure 8).

When the successive extreme events are very close (<3 tides), the [SPMC]index is the lowest, reaching values between 0.7 and 0.9. When events are separated by at least 5 tides, the [SPMC]index values are mainly above 0.9, indicating significant settling. These results illustrate a memory effect of extreme events, keeping SPMC to high levels up to ~3 tides after the event.

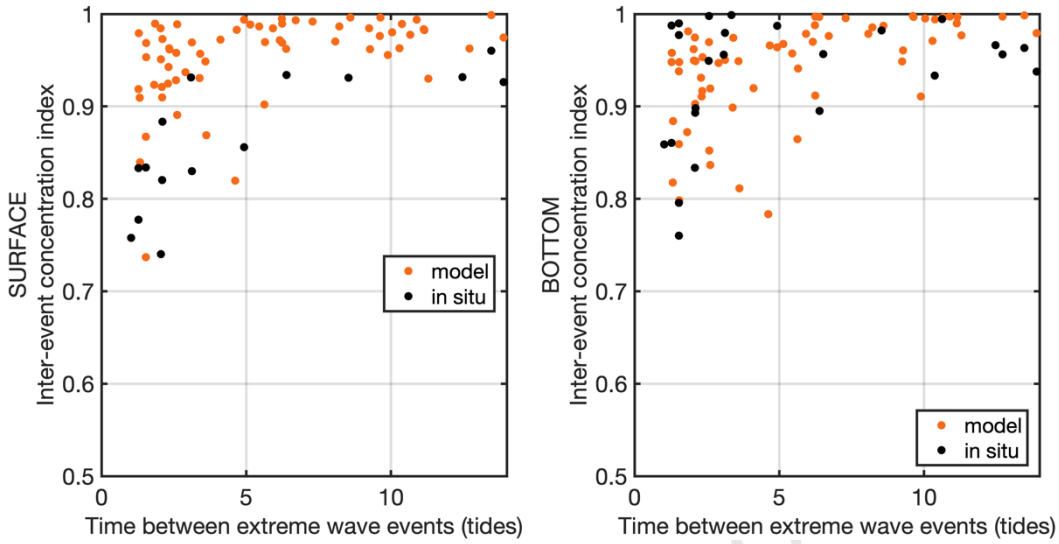

Figure 8 : Relation between the time (tides) between 2 consecutive extreme wave events and the inter-event concentration index ([SPMC]index). Surface data (left) and bottom data (right). Black circles represent *in situ* data and orange circles model data.

3.3 Spatial extent of SPMC during extreme river flow and wave events

3.3.1 Spatial response to extreme river flow events: investigating the SPM surface plume dynamics

In order to complement the local influence of extreme events observed from coastal observatories, the surface SPMC evaluated from satellite ocean color data can be analyzed to investigate the spatial dimension of these events. Hence, the sediment surface plume area is calculated after averaging available images every 15 days from the beginning to the end of each event (Figure 9, 10 and 11). Three specific examples are first studied below.

First, we consider the weakest and shortest extreme flood event (1.2 times the smoothed P90 threshold) from mid-September to mid-October 2008 (Figure 9). A rounded plume faces the Seine estuary close to the mouth as it does not extend further 0.05°W. This late summer extreme flow event is characterized by a low river discharge around 400m^3 s^{-1} and low waves

(average square wave orbital velocities below 0.2m^2 s^{-2}). This situation explains the weak evolution of the sediment plume during the event.

Secondly, the opposite extreme situation is studied with the longest and strongest extreme flood event occurring from January to May 2018 (Figure 10). The sediment surface plume is highly spread out in January with a plume that exceeds West of 0.3°W and North of 49.7°N during the first half of the event (brown and yellow shades). Then the plume gradually moves closer to the estuary mouth with a boundary around 0.15°W (red shades) as the river discharge decreases. It can be seen that the evolution of the SPMC contour is important between each 15-day period. This event, which is divided into two phases, presents first a very important flood peak higher than 2000m^3 s^{-1} but also important waves with square wave orbital velocity peaks higher than 0.5m^2 s^{-2} and followed next by lower conditions of river flows (less than 1300m^3 s^{-1}) and low square wave orbital velocities below 0.2m^2 s^{-2}.

Finally, the rarest event is examined (Figure 11): it is the second most intense extreme event (up to 2000m^3 s^{-1}) which happens in summer 2016, a season in which such high discharge is unexpected. Similarly to the strongest event, the sediment surface plume is present in the bay up to 0.15°W when the peak river flow is observed. The weak North wind favors an extension of the SPM surface plume towards the West, confined close to the coast. Then rapidly after 15 days, the plume extension is progressively reduced and centered close to the mouth, around 0.05 to 0.1°W, as expected during medium to low river flow conditions. This event presents a sudden and very intense peak of river flow close to 2000m^3 s^{-1} and does not present any concurrent impact of waves, which are weak all the time during the event (square wave orbital velocities below 0.25m^2 s^{-2}). Such an event in a dry period field to a rapid response of the system.

We can conclude that the extent of the SPM surface plume is strongly driven by the intensity and duration of the event. The evolution of the SPM surface plume is rapid and

important in winter while it is smaller and slower in summer. It can be remembered that the wave effect is not distinguishable from the river flow effect from SPM surface satellite observations.

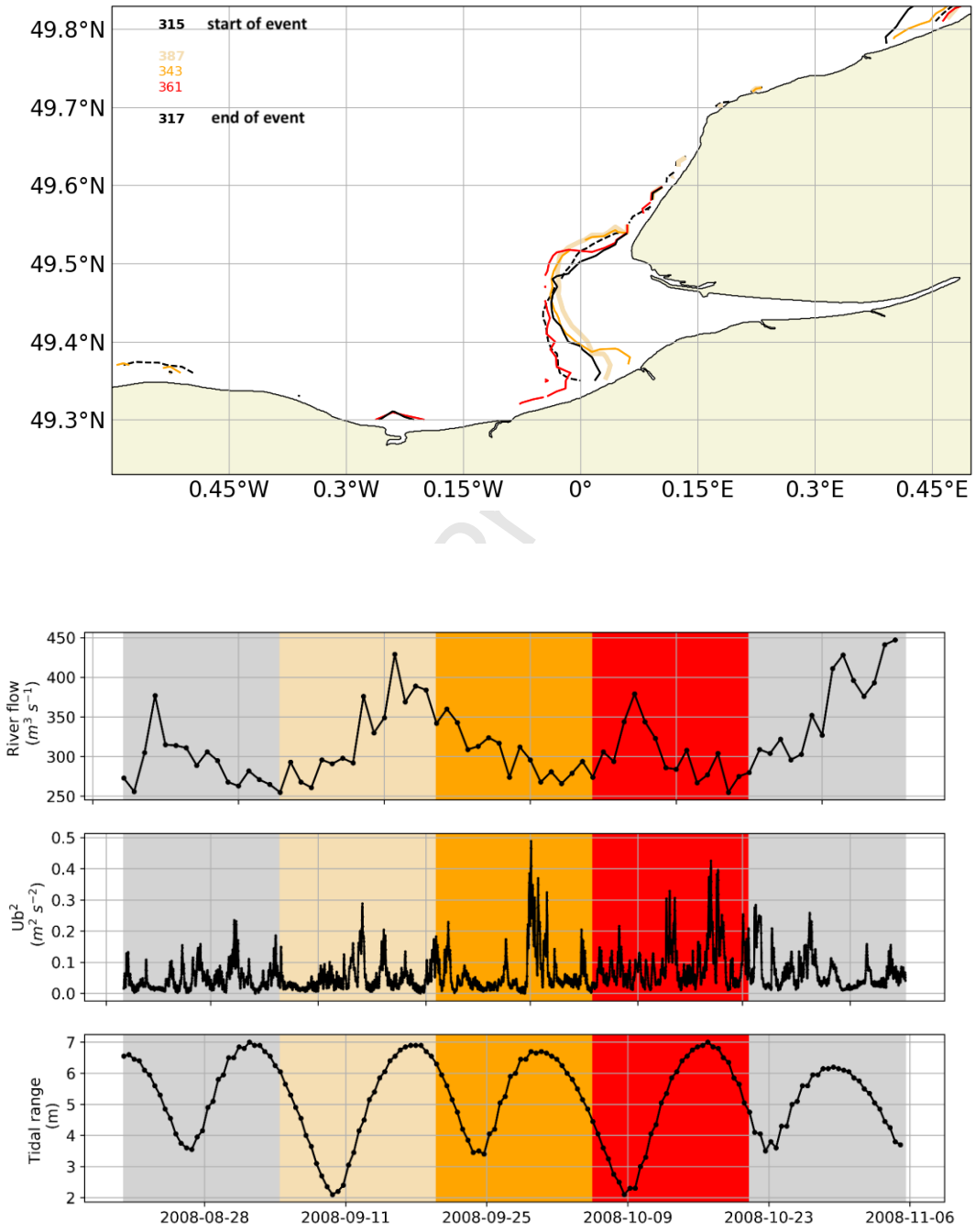

Figure 9 : Evolution of the SPM surface distribution represented by the 5 mg L^{-1} SPMC contour every 15 days for the weakest event in early autumn 2008 (top) and corresponding forcing time series: river

discharge, square wave orbital velocity and tidal range (bottom). Contour color lines correspond to shaded contours in the bottom panel.

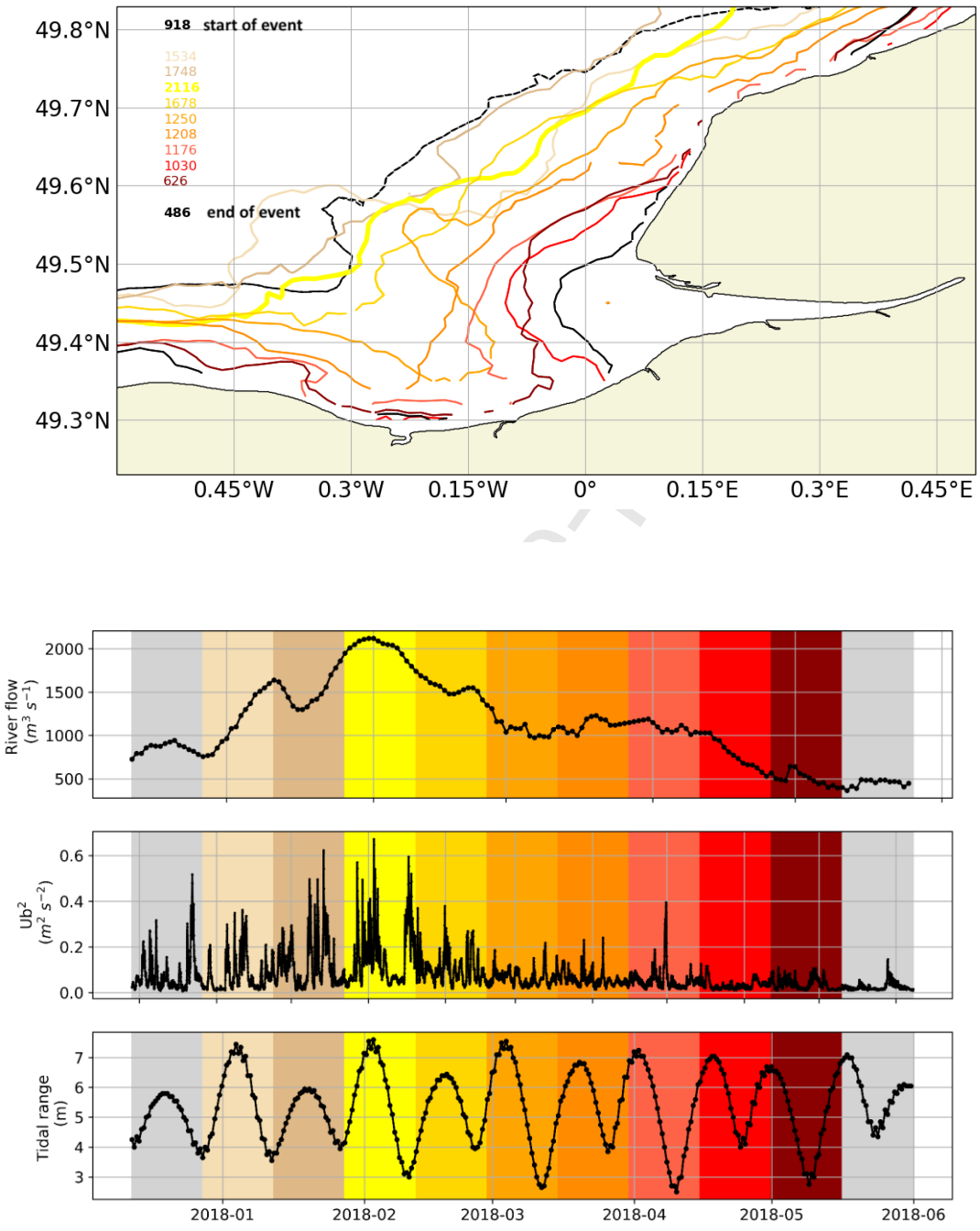

Figure 10 : Evolution of the SPM surface distribution represented by the 5 mg L^{-1} SPMC contour every 15 days for the strongest event in winter 2018 (top) and corresponding forcing time series: river discharge, square wave orbital velocity and tidal range (bottom). Contour color lines correspond to shaded contours in the bottom panel.

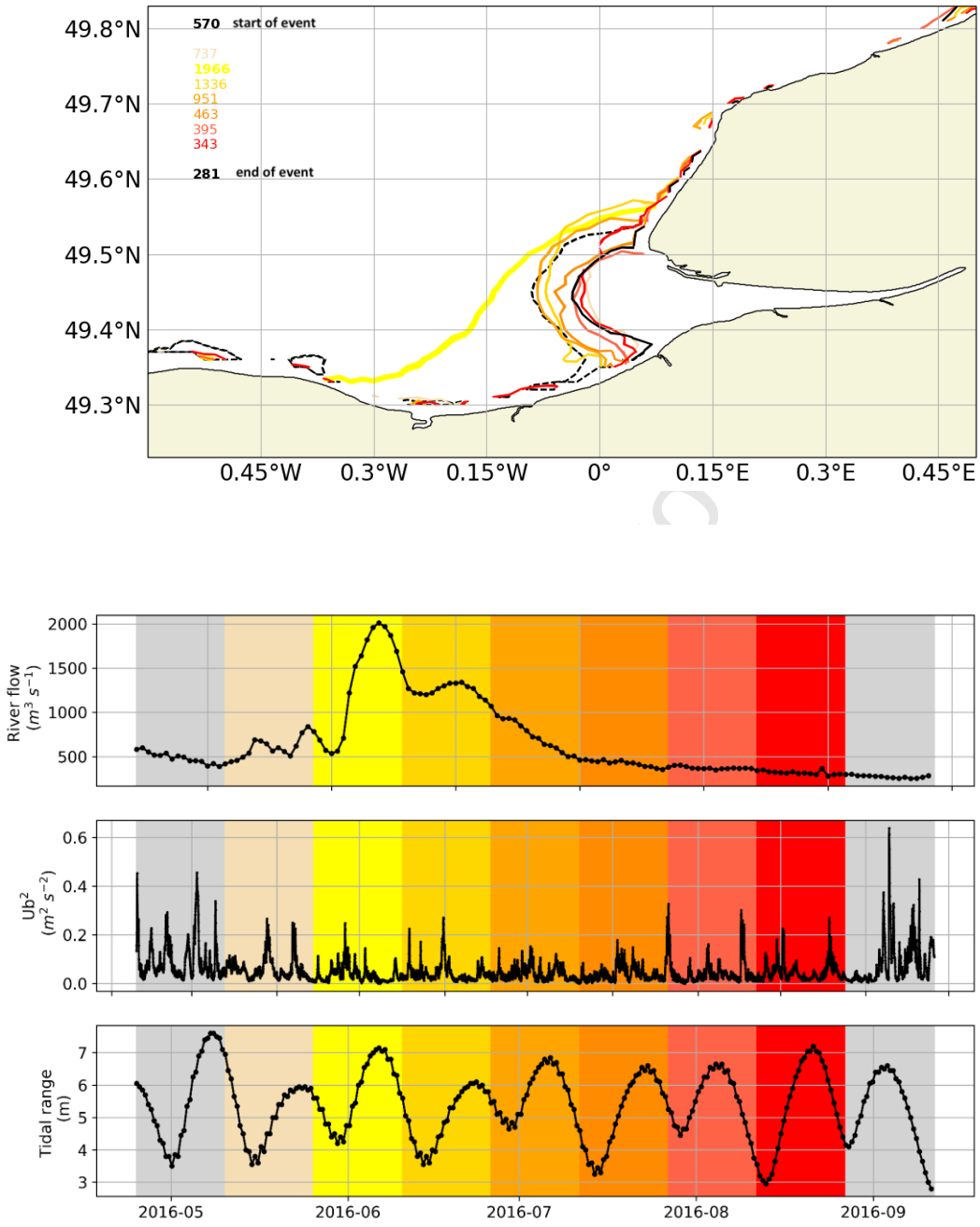

Figure 11 : Evolution of the SPM surface distribution represented by the 5 mg L^{-1} SPMC contour every 15 days for the rarest event in summer 2016 (top) and corresponding forcing time series: river discharge, square wave orbital velocity and tidal range (bottom). Contour color lines correspond to shaded contours in the bottom panel.

Next, all events are considered and SPM surface plumes are confronted to extreme river flow values, in order to examine general patterns of plume shapes in response to river flow (Figure 12).

For each extreme flood event, the date of the maximum river flow is identified and the satellite images that correspond to the week following this date are selected to compute a mean image and calculate the corresponding area with SPMC larger or equal to 5mg L^{-1}. A general pattern is reported, with increasing SPMC surface plume area (up to 80% of the studied area) with increasing river flow values (Figure 12). Low-intensity extreme river flow yield to a sediment plume that remains close to the river mouth and covering less than 25% of the area (for $Q<600m^3\ s^{-1}$).

Some SPMC plume associated to high river flow values ($Q>1600m^3\ s^{-1}$) show low turbid area values. This could be explained by the impact of wind on surface flow and pushing the plume toward the coast, as observed by Gangloff et al. (2017) in the Rhone river plume.

3.3.2 Understanding the spatial distribution of surface SPMC in response to wave extreme events

SPMC satellite L4 products are averaged by wave events to examine how extreme events spatially impact the estuary-sea interface. The SPMC surface area (pixels where SPMC exceed 5mg L^{-1} divided by the total sea pixels in the studied area), are concurrently analyzed with U_b^2 and the river flow (Figure 12).

The relation between the SPMC and the wave intensity shows a positive trend: the larger the wave intensity, the more spread the spatial distribution of surface SPMC. For event-average square orbital velocities lower than $0.1m^2\ s^{-2}$, the high SPM area (where SPMC is above 0.005g L^{-1}) covers between 10% to 60% of the studied area. When U_b^2 exceed $0.2m^2\ s^{-2}$, the high SPMC

area increases from 30% to 95%. Together with the spatial extent, the SPMC within the turbid plume can be investigated (Figure 12). When the wave event intensity increases, the percentile 90 of SPMC within the detected plume increase. For low intensity events ($U_b^2 < 0.1 m^2 s^{-2}$), the average P90 SPMC values reaches 0.025g L^{-1} while it reaches 0.050g L^{-1} for U_b^2 larger than $0.2 m^2 s^{-2}$. We can also note that the plume extent also increases with the river flow, as highlighted in section 3.3.1.

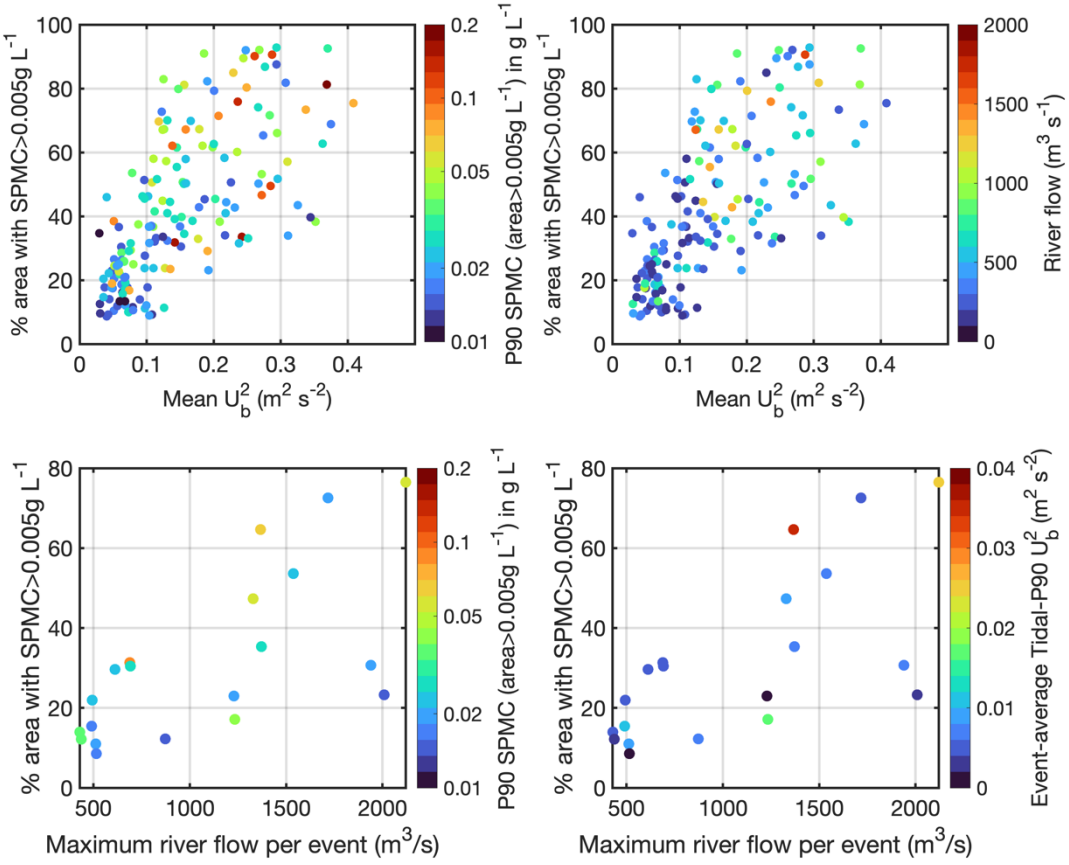

Figure 12 : Percentage of surface SPMC areas (pixel values >superior to 5mg L^{-1}) in relation to extreme event characteristics. Top panel: wave extreme events characterized by event-average U_b^2. The color bar on each panel shows: left) the percentile 90 of the SPMC within the selected turbid area; right) the corresponding river flow. Bottom panel: river flow extreme events characterized by the maximum river flow. The color bar on each panel shows: left) the percentile 90 of the SPMC within the selected turbid area; right) the corresponding mean tidal-P90 wave orbital velocity per event.

4. Discussion

4.1 Reversal of the extreme detection method: exploring SPMC extreme events

In this study the extreme wave and river flow events are detected and the associated SPMC response was then analyzed. This is the usual strategy used in previous studies to observe the impact of extreme external hydro-meteorological events such as storms (Fettweis *et al.*, 2010) and floods (Tavora *et al.*, 2023) on SPMC. Meanwhile, questions can arise if a direct cascade effect exists, and if an extreme event in the forcing necessarily implies an extreme event in SPMC anomalies. Both methods, (i) the detection of extreme forcings and response in SPMC and (ii) the detection of extreme SPMC are compared to analyze the possible concomitance and mismatches. This is tested on modelled (longest, continuous) SPMC anomaly time series from 2006 to 2019 at the surface and at the bottom using the same methodology as applied for observations (Verney *et al.*, 2024). The results show a good agreement between both detection methods with a similar number of events. 234 SPMC anomaly extreme events are found at the surface and 175 at the bottom against 155 wave extreme events detected over the same period (2006-2019). Also, differences are observed on the number of non-detected extreme events (Figure 13). There are 63% of surface SPMC anomaly extreme events detected in model data that do not correspond to extreme wave events, against also 42% wave extreme events that do not correspond to extreme SPMC anomalies at the surface. The same patterns are observed for bottom SPMC anomaly analysis with 52% SPMC anomaly extreme events not concomitant with wave extreme events and 43% wave events not concomitant with SPMC anomaly events. Investigating further these mismatches between extreme events, the non-detected wave extreme events (within the SPMC anomaly extreme event) (Figure 13 right panels) correspond to low wave intensity events (below $0.2 m^2 s^{-2}$). Moreover, the most intense ones ($>0.05 m^2 s^{-2}$) are reported in winter, when wave activity

and the resulting P90 U_b^2 climatology are usually high (i.e. > 0.15m^2 s^{-2}), hence explaining why these events are not detected as extreme in the wave time series. Similar patterns are observed for wave extreme events not detected as extreme in the SPMC anomaly time series (both surface and bottom): these non-detected events are characterized by low SPMC anomaly values, far from the P90 climatology threshold whatever the season. This is particularly atypical in winter, when wave extreme events reach values higher than 0.2m^2 s^{-2}, but not generating high sediment resuspension. This could be explained by less fine sediment available at the sediment surface or weaker erosion rates. It must be reminded here that model results are examined here, and this behavior might be strongly controlled by the erosion rate calculation, strongly driven by the sand fraction (Le Hir et al., 2011; Grasso et al., 2018)

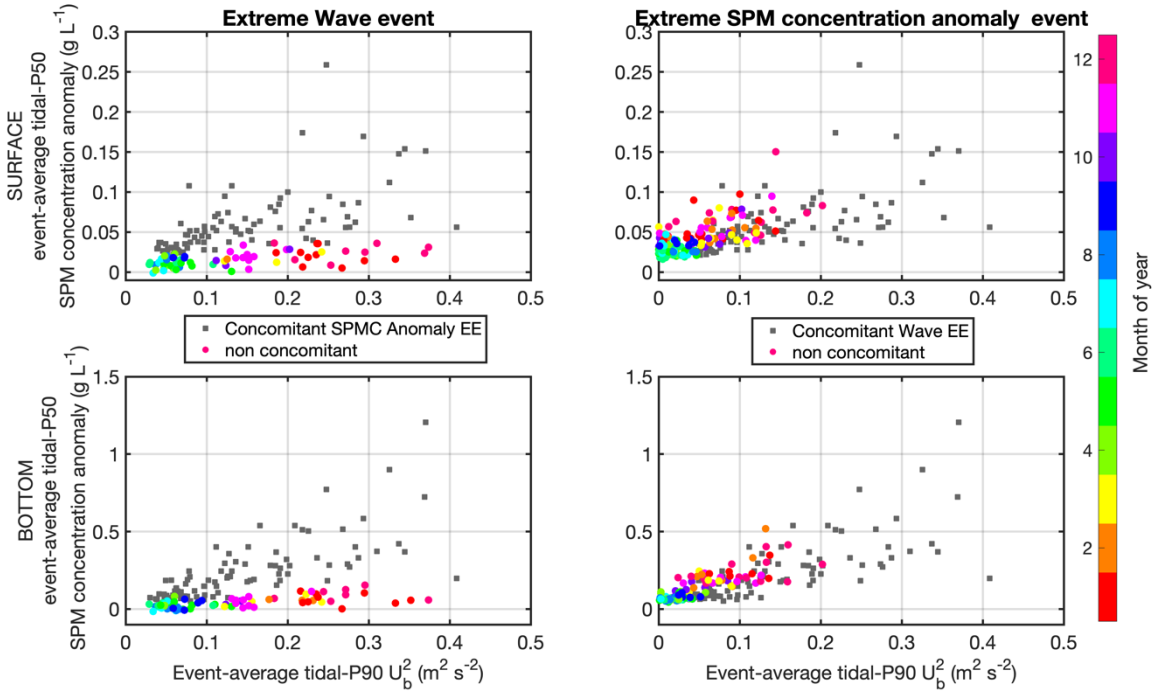

Figure 13 : Exploring the concomitance of extreme wave events and model extreme SPMC anomaly event (Top: surface; Bottom: bottom). Each panel indicates the concomitance (grey squares) and absence of concomitance (circles) between extreme events. The color bar represents the month of the year of the extreme event. The left panel examines the possible concomitance of SPMC anomaly events for all extreme wave events, and inversely for the right panel.

4.2 Robustness of the extreme detection method: the threshold question

In a second step, the robustness of our method is questioned as well as the definition of extreme events. SPMC response to extreme wave forcing is often investigated for specific events and generally during the winter season when storms are strongest (Warner *et al.*, 2008; Lettmann *et al.*, 2009; Fettweis *et al.*, 2010). In this study, 29 extreme river flow events and 287 extreme wave events are detected over less than 2 decades from 2006 to 2022 during all seasons.

The choice for using the percentile 90 as a threshold is questionable. The percentile 90 remains the most used threshold in the scientific community (McPhillips *et al*., 2018), as used in marine heatwaves studies (Hobday *et al*., 2016). The percentile 95 is used to detect extreme events of river flows and significant wave heights in the Bay of Seine by Grasso *et al*. (2021), or intense hydrodynamic events in the mudflat of the Gironde region by Lamarque *et al*. (2022) and extreme river flows and winds in the Scheldt estuary by Tavora *et al.* (2023). Our method seems to be robust with both thresholds (percentile 90 versus percentile 95) giving similar results (Figure 14). The same events are (generally) detected, while (10 to 25%) fewer events are detected with a higher percentile, as mathematically expected. The threshold chosen will depend on the scientific question, whether it concerns the determination of a trend of these extremes considered as rare or whether, as in our case, the interannual variability and the processes related to these extremes are studied.

Another aspect of this method is the temporal variability of the threshold which is also to be taken into account according to the scientific question investigated. In a (simple) physical study context, it could be studied only during the winter period, for example, when storms are

the most important (Poppeschi *et al.*, 2021). On the other hand, if the study ambitions to investigate different compartments of the ecosystem, it will be necessary to extend the study over the year or over a season that is more favorable to the observation of these biological processes. The threshold can be either fixed to a standard value (e.g. as for oxygen - Conley *et al*., 2009) or variable in time (Stephenson, 2008). For the latter, thresholds can be fixed or can vary according to a certain frequency: tide, month or season (Figure 14). Marine heatwaves for example are generally only studied in summer with a seasonal threshold calculated from a daily climatology (Hobday *et al*., 2016) but with climate change, these extreme phenomena studies could be extended to the months surrounding the summer season as well. Because of global change, extremes are more and more present during unexpected periods, and it is mandatory to study them using variable thresholds with the finest possible temporal resolution in order to detect all extreme events all year long, as proposed in the present study.

The integration time period to calculate the threshold plays a role in detecting extremes. Climate scientists recommend estimating a threshold over a period of at least 30 years (Hobday *et al.*, 2016; Oliver *et al*., 2008). However, present *in situ* data rarely cover such long periods of time, especially at high frequencies. Some series exceed 30 years like the Hawaii ocean time-series (HOT, Karl and Lucas, 1996), but most are shorter than a decade or limited to several years (Poppeschi *et al.*, 2022). The time series of physical forcing are often longer because they have been collected and archived by specialized organizations for decades such as Météo-France for meteorological parameters or the Shom for tides in France. Therefore, tests are performed in this study on the Seine River flows for threshold computed based on 10 to 60years of data and for waves in the Bay of Seine over 5 to 25years of data (Figure 14). The integration time period implies a variability in the calculated threshold, but these variations are weak compared to other methodological parameters such as the percentile value or the threshold

variability time scale. We also examine if splitting the signal in small time periods would not lead to the same conclusions as on a longer period (not shown), and results do not differ much as well.

(a)

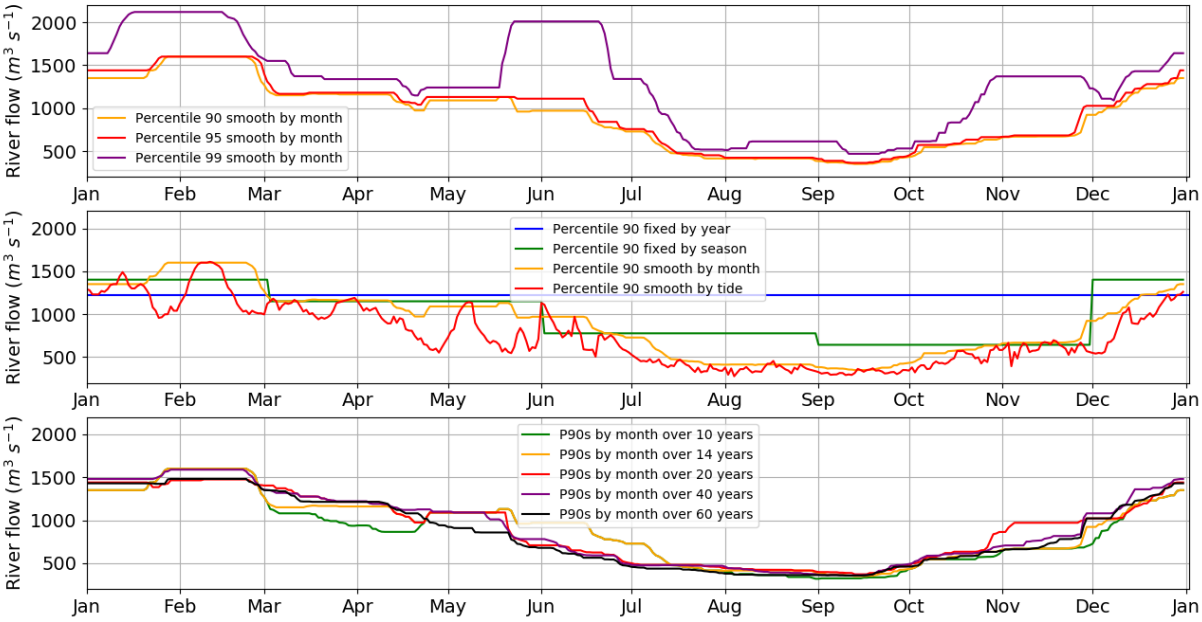

(b)

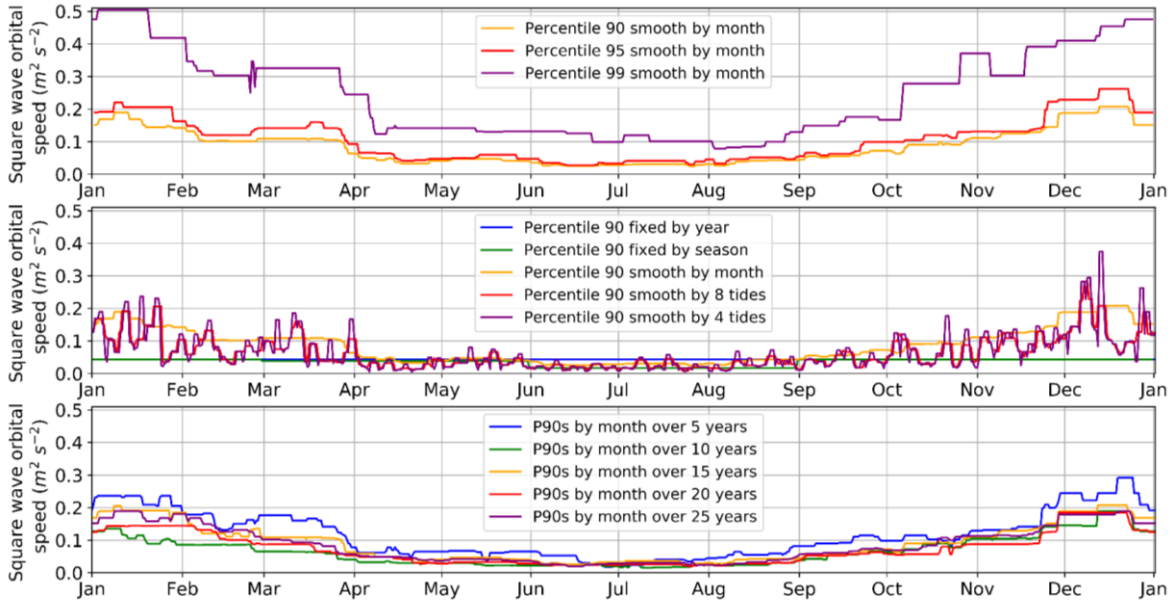

Figure 14 : Analysis of thresholds for the extreme event detection method over percentiles, temporal variability and duration period on (a) river flow and (b) waves

4.3 Examining the impact of extreme events against the seasonal dynamics

From previous results and Figure 7 and 12, we may conclude that extreme events (both river flow and wave events) impacting the most system are the most intense ones, as they result on the largest SPMC anomalies or the largest surface SPMC areas. However, it is essential to contextualize these impacts along the seasonal dynamics of the SPMC anomalies (Figure 15). Hence considering extreme wave events, the event-average SPMC anomaly can be compared with the monthly interannual SPMC anomaly statistics. Examining bottom data, winter (December to February) wave events generate SPMC anomalies that range from 0.025 to 0.15g L^{-1}, while the percentile 90 of the monthly interannual SPMC anomaly reaches at this period on average 0.08g L^{-1}. Extreme events SPMC anomalies are mainly less than twice higher the percentile value. In April and May, SPMC anomalies induced by an extreme event range from 0.02 to 0.08g L^{-1}, while the monthly interannual percentile 90 value reaches 0.015g L^{-1} on average. During the spring period, the extreme events induce SPMC anomalies that can be more than 4 times the monthly interannual percentile 90 value. Similar results are observed during summer and at the surface, indicating that if their intensities are lower, the extreme wave events in spring and summer also significantly impact the estuary-bay system. Considering extreme river flow events, their impact is globally not significant, despite slightly higher median anomalies than the monthly interannual median value. For these events, and only considering the sediment dynamics at the estuary-bay interface, exceptionally intense events, such as the event recorded in June 2016, are expected to significantly impact the SPMC at the mouth and in the bay nearby.

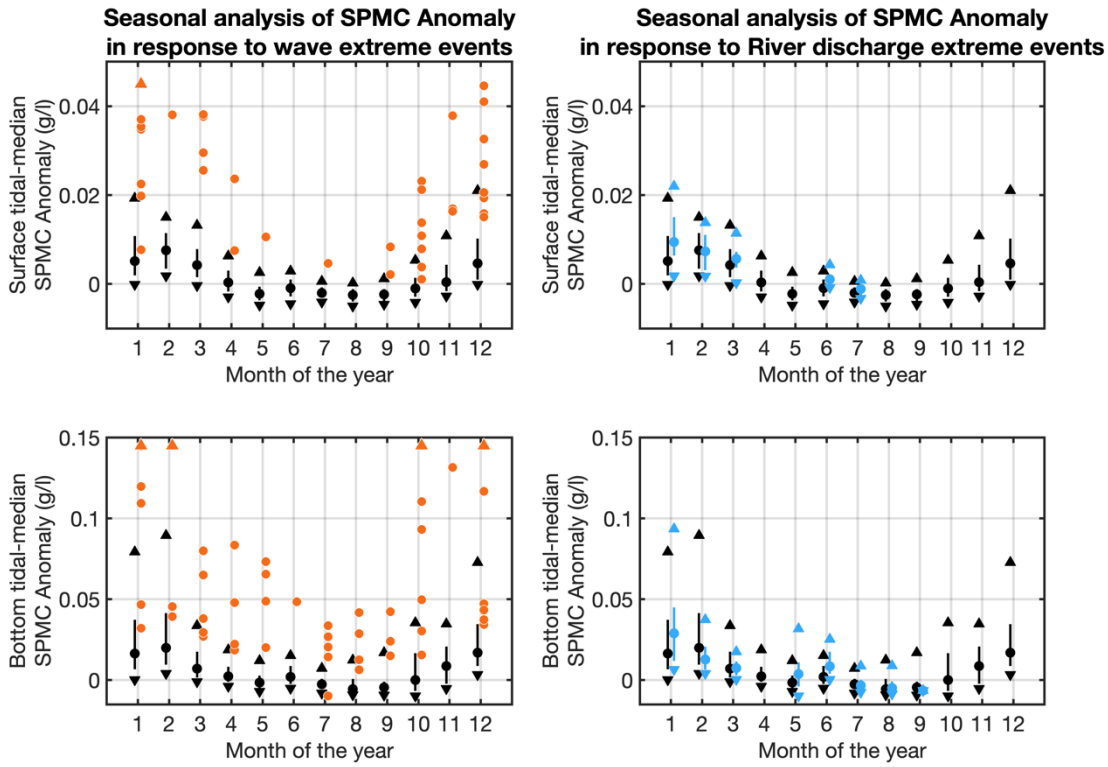

Figure 15 : Comparison between monthly SPMC anomaly climatology and the seasonal SPMC anomaly in response to extreme events. Left: wave events, Right: river flow events. Top panel: surface, Bottom panel: bottom. Climatology anomalies are represented by black markers and lines: circles show the monthly median anomaly, lines indicate the percentile 25 and 75, up and down triangles the percentile 90 and percentile 10 respectively. Orange circles represent event-average tidal-median SPMC anomalies. Up orange triangles indicate high SPMC anomalies above 0.05 and 0.15g L^{-1} for surface and bottom data respectively. Blue markers and lines indicate the monthly distribution of SPMC anomalies during extreme river flow events (similarly to SPMC anomalies)

4.4 Variability of extreme river flow events over a 60-year period

Extreme hydro-meteorological events are intensifying worldwide, becoming larger in magnitude and more frequent in occurrence implying important consequences for coastal ecosystems (Breitburg *et al.*, 2018; Ibrahim *et al.*, 2021; IPCC, 2021). This assumption is investigated in this section, evaluating temporal variability of extreme river flow events over the 1962-2022 period (hence the percentile 90 threshold was recalculated over this period)

(Figure 16). A general trend is observed, the occurrence of river flow extreme events increasing from the 1960th to the 2010th: from 1962 to 1981, 22 events are detected, against 40 from 2002 to 2021. All river flow event classes increase, but low river flow extreme events (Q<500m^3 s^{-1}) more than double (from 4 to 11 occurrences). The number of short events (T<20days) increases the most, from 10 to more than 20 events, but still all classes show an increase in occurrences from 1962-1981 to 2002-2021. This is in agreement with predictions, which anticipate that extreme events should be more important and stronger. But quantitative comparison with other studies is complicated as the methodology used to define and detect extreme events often differ. There are many different methods to examine river flow extreme events (Garner et al., 2015), and this could contribute to significantly bias their representation. Also, it can be reported a pluri-decadal variability in the occurrence of extreme river flow event, with more event detected from 1982-2001 than for the following period (51 Vs 41 events), and especially for the most intense events (Q>1000m^3 s^{-1}). This can be explained by decadal climatic variability as discussed in Garner et al. (2015) or Jalon Rojas and Castelle (2021).

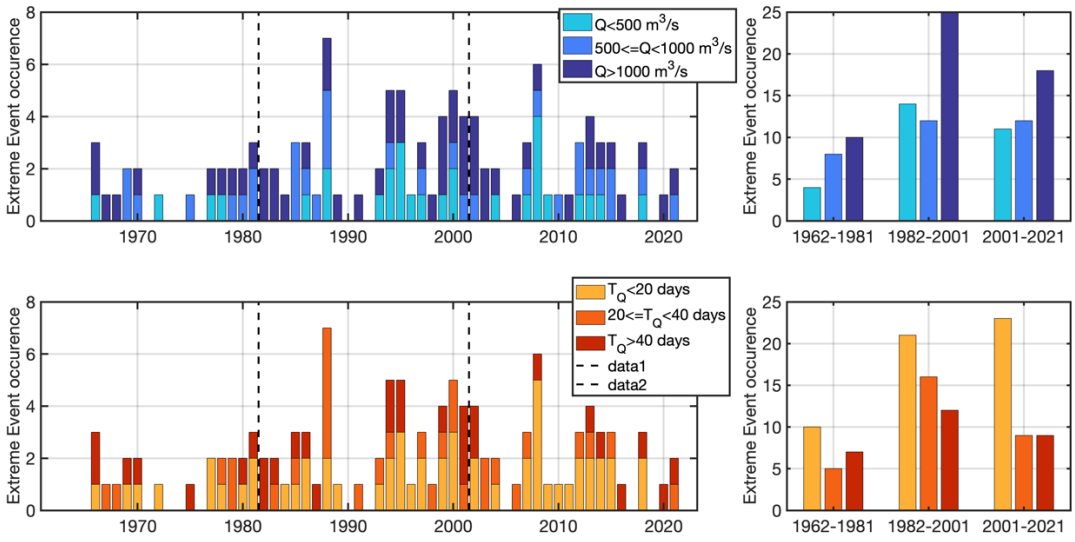

Figure 16 : Annual statistics of extreme river flow events from 1962 to 2022 (each year is considered as the hydrological year, i.e. from September Year-1 to August Year). Occurrences of extreme event

by three maximum river flow classes per year (a) or per 20y-periods (b). Occurrences of extreme events per event duration classes (days) per year (c) or per 20y periods (d). The dashed lines in a and c indicate the separation between the three 20y-periods

Together with a general increase in occurrences over decades, the event seasonality per 20y-periods can be further discussed (Figure 17). On one hand, similar patterns of events are observed in January/February (high river flow) and July to October (low river flow), in terms of intensities and number of occurrences. On the other hand, differences are reported during spring/early summer. High extreme events ($Q>900m^3\ s^{-1}$) are not reported in the 1962-1981 period (April and May), while 7 were observed in April/early May in 1982-2021 and 5 in May/June in 2002-2021. This time shift within the spring period is impacting, as recent (2002-2021) extreme events in May/June are as intense as in April but occurring during lower river flow period, hence generating potentially higher gradients in SPMC at the estuary/sea interface with potentially stronger impact on the biological compartment of the estuarine and coastal ecosystem. A similar seasonal shift was also observed in northern and eastern US and Canadian river systems as reported by Dethier et al. (2020).

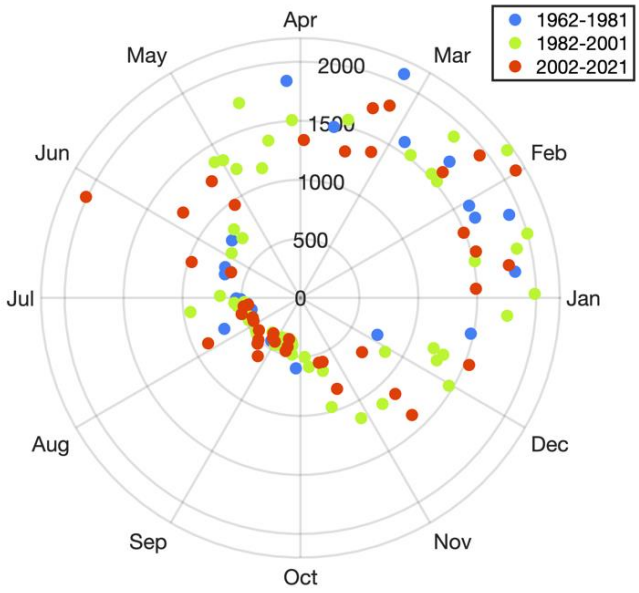

Figure 17 : Monthly variability of extreme river flow event distribution per 20y periods: 1962-1981; 1982-2021; 2002-2021. Radial values indicate the river flow ($m^3\ s^{-1}$)

5 Conclusion

Extreme hydro-meteorological events playing a role in sediment dynamics at the mouth of the Seine estuary have been detected using an innovative detection method applied to long term high frequency time series. This method investigates extreme wave and river flow events occurrence throughout the years, can be easily transposed to other coastal and estuarine sites, and its robustness has been validated in this study. From 2006 to 2022, 20 river flow events and 211 wave extreme events were detected. A strong seasonality of these extreme events is highlighted with highest intensity and more successions of events in winter. The pluri-decadal change in extreme river flow event was investigated and showed an increase in occurrences in river flow extreme event from 1962-1981 to 2002-2021. Over the last 40years (1982-2021), intense river extreme events are reported during atypical, low mean river flow periods (April to June) that were not detected from 1962 to 1981, illustrating a shift that could be a consequence of climate change.

The SPMC response to extreme events is analyzed through tidal anomalies time series and satellite ocean color SPM surface concentration data. In general, the more intense the event, the larger the SPMC or the larger the high concentration spatial extent, whatever the type of event. Extreme wave events are the most impacting, generating large anomalies (stronger near the bottom than close to surface) than river flow extreme events. During summer, the average lower intensity of extreme wave or river flow events leads to lower SPMC anomalies. However, considering wave events, these anomalies in late spring and summer are up to 4times larger than the mean monthly anomaly, hence potentially significantly impacting as much the coastal ecosystem as winter high intensity storms. Extreme river flow events also generate statically larger SPMC anomalies than the climatology values, but lower than wave events. However,

exceptional extreme high intensity river events in late spring/summer, such as observed in June 2016, can greatly increase SPMC anomalies at the estuary-sea interface.

Based on the annual SPMC anomaly distribution, extreme wave events do not necessarily induce extreme SPMC anomalies (~40%). Mismatches in extreme events (forcing Vs SPMC anomalies) is explained by their seasonality: low intensity wave events in summer induce low shear rate and hence low SPM resuspension, not necessary detected as extreme in the SPMC signal. High intensity wave extreme events not detected as extreme in SPMC anomalies occur all in winter, a season when SPMC anomalies are already high on average.

The importance of adapting the method for studying extremes to the parameter was discussed. The various tests carried out have shown that the choice of threshold, its variability and the duration of its application are parameters to be considered and adapted according to the research question.

Because waves and river flows are not the only forcings playing a role on SPM dynamic, biological effects on flocculation and bed erodibility need also to be considered in future studies. It would also be interesting to extend this study by considering the interactions between SPMC and phytoplankton in the Bay of Seine.

6 Open data

All data used in this manuscript will be publicly available.

Model data are accessible here : ftp://ftp.ifremer.fr//ifremer/dataref/ocean-coastal-model/SEINE/curviseine_ares_hindcast/

L4 satellite data are accessible from httpd://marc.ifremer.fr/en.

In situ data are partly available from https://coast-hf.fr/. A DOI will be provided before publication.

7 Acknowledgments

This study is part of the Contrat Plan Etat-Region ObsOcean / ROEC-ILICO and the COXTCLIM project funded by the Loire-Brittany Water Agency, the Brittany region, and Ifremer. This study also contributes to the RUNTIME project, co-funded by the EC2CO program and OFB and the PHRESQUES2 project, funded by the CPIER Vallée de Seine and coordinated by the GIP Seine Aval.

We would like to acknowledge the COAST-HF (http://www.coast-hf.fr) national observing network component of the National Research Infrastructure ILICO. We would like to thank the Shom for tidal data and Météo-France for wind products. Finally, we are grateful to Anne Daniel of the Pelagos laboratory at Ifremer in Brest, France for her constructive comments and her attentive review of this article.

8 References

Aminot, A., Guillaud, J-F., Kerouel, R., 1997. La baie de Seine : hydrologie, nutriments, chlorophylle (1978-1994). Repères océans, 14, 151.

Artelia, 2019. Définition des périodes de retour des forçages et des niveaux de pleines mers en estuaire de Seine pour la gestion du risque inondation. Rapport réalisé pour le GIP Seine-Aval et la DREAL Normandie, 99.

Breitburg, D., Levin, L.A., Oschlies, A., Grégoire, M., Chavez, F.P., Conley, D.J., Garçon, V., Gilbert, D., Gutiérrez, D., Isensee, K., Jacinto, G.S., Limburg, K.E., Montes, I., Naqvi, S.W.A., Pitcher, G.C., Rabalais, N.N., Roman, M.R., Rose, K.A., Seibel, B.A., Telszewski, M., Yasuhara, M., Zhang, J., 2018. Declining oxygen in the global ocean and coastal waters. Science, 359(6371). https://dx.doi.org/10.1126/science.aam7240.

Burchard, H., Schuttelaars, H.M., Ralston, D.K., 2018. Sediment trapping in estuaries. Annu. Rev. Mar. Sci., 10, 371-95. https://doi.org/10.1146/annurev-marine-010816-060535.

Cailleaud, K., Forget-Leray, J., Souissi, S., Hilde, D., LeMenach, K., Budzinski, H., 2007. Seasonal variations of hydrophobic organic contaminant concentrations in the water-column of the Seine Estuary and their transfer to a planktonic species Eurytemora affinis (Calanoïda, copepoda). Part 1: PCBs and PAHs. Chemosphere, 70(2), 270-280. https://doi.org/10.1016/j.chemosphere.2007.05.095.

Chen, M., Li, F., Tao, M., Hu, L., Shi, Y., Liu, Y., 2019. Distribution and ecological risks of heavy metals in river sediments and overlying water in typical mining areas of China. Marine Pollution Bulletin, 146(March), 893–899. https://doi.org/10.1016/j.marpolbul.2019.07.029.

Cheng, P., Li, M., Li, Y., 2013. Generation of an estuarine sediment plume by a tropical storm. Journal of Geophysical Research: Oceans, 118(2), 856–868. https://doi.org/10.1002/jgrc.20070.

Cocquempot, L., Delacourt, C., Paillet, J., Riou, P., Aucan, J., Castelle, B., Charria, G., Claudet, J., Conan, P., Coppola, L., Hocdé, R., Planes, S., Raimbault, P., Savoye, N., Testut, L., Vuillemin, R., 2019. Coastal ocean and nearshore observation: A French case study. Front. Mar. Sci., 6, 324. https://doi.org/10.3389/fmars.2019.00324.

Cloern, J., 1987. Turbidity as a control on phytoplankton biomass and productivity in estuaries. Continental Shelf Research, 7(11-12), 1367-1381. https://doi.org/10.1016/0278-4343(87)90042-2.

Conley, D.J., Carstensen, J., Vaquer-Sunyer, R., Duarte, C. M., 2009. Ecosystem thresholds with hypoxia. In Eutrophication in Coastal Ecosystems: Towards better understanding and management strategies Selected Papers from the Second International Symposium on Research and Management of Eutrophication in Coastal Ecosystems, (20–23), 21-29. https://doi.org/10.1007/s10750-009-9764-2.

Deloffre, J., Lafite, R., Lesueur, P., Lesourd, S., Verney, R., Guézennec, L., 2005. Sedimentary processes on an intertidal mudflat in the upper macrotidal Seine estuary, France. *Estuar. Coast. Shelf Sci.*, *64*(4), 710-720. https://doi.org/10.1016/j.ecss.2005.04.004.

Dufois, F., Verney, R., Le Hir, P., Dumas, F., Charmasson, S., 2014. Impact of winter storms on sediment erosion in the rhone river prodelta and fate of sediment in the gulf of lion (north western Mediterranean sea). Cont. Shelf Res., 72, 57-72. https://doi.org/10.1016/j.csr.2013.11.004.

Fan, J., Fan, D., Wu, Y., 2023. Spatiotemporal variations of heavy metal historical accumulation records and their influencing mechanisms in the Yangtze River Estuary. Science of the Total Environment, 854(June 2022), 158733. https://doi.org/10.1016/j.scitotenv.2022.158733.

Farcy, P., Durand, D., Charria, G., Painting, S. J., Tamminen, T., Collingridge, K., Gremare, A., Delauney, L., Puillat, I., 2019. Toward a European coastal observing network to provide better answers to science and to societal challenges; the JERICO research infrastructure. Front. Mar. Sci., 6, 529. https://doi.org/10.3389/fmars.2019.00529.

Fettweis, M., Francken, F., Van den Eynde, D., Verwaest, T., Janssens, J., Van Lancker, V., 2010. Storm influence on SPM concentrations in a coastal turbidity maximum area with high anthropogenic impact (southern North Sea). Cont. Shelf Res., 30(13), 1417-1427. https://doi.org/10.1016/j.csr.2010.05.001.

Figueiredo, B. R. S., Calvo, C., López-Rodríguez, A., Mormul, R. P., Teixeira-de Mello, F., Benedito, E., Meerhoff, M., 2019. Short-term interactive effects of experimental heat waves and turbidity pulses on the foraging success of a subtropical invertivorous fish. Water, 11(10), 1–13. https://doi.org/10.3390/w11102109.

Gangloff, A., Verney, R., Doxaran, D., Ody, A., Estournel, C., 2017. Investigating Rhône River plume (Gulf of Lions, France) dynamics using metrics analysis from the MERIS 300 m Ocean Color archive (2002-2012). Cont. Shelf Res., 144, 98-111. https://dx.doi.org/10.1016/j.csr.2017.06.24

Garner, G., Van Loon, A.F., Prudhomme, C., Hannah, D.M., 2015. Hydroclimatology of extreme river flows. Freshwater Biology 60, 2461–2476. https://doi.org/10.1111/fwb.12667

Gohin, F., 2011. Annual cycles of chlorophyll-a, non-algal suspended particulate matter, and turbidity observed from space and in-situ in coastal waters. Ocean Sci., 7(5), 705-732. https://doi.org/10.5194/os-7-705-2011.

Grasso, F., Le Hir, P., Bassoullet, P., 2015. Numerical modelling of mixed-sediment consolidation. Ocean Dyn., 65(4), 607-616. https://doi.org/10.1007/s10236-015-0818-x.

Grasso, F., Verney, R., Le Hir, P., Thouvenin, B., Schulz, E., Kervella, Y., Khojasteh Pour Fard, I., Lemoine, J.-P., Dumas, F., Garnier, V., 2018. Suspended sediment dynamics in the macrotidal Seine Estuary (France): 1. Numerical modeling of turbidity maximum dynamics. J. Geophys. Res. Oceans, 123(1), 558-577. https://doi.org/10.1002/2016JC012638.

Grasso, F., Bismuth, E., Verney, R., 2020. Projet Seine-Aval 6 ARES « Analyse de Rejeux hydro-sédimentaires en Estuaire de Seine ». GIP Seine-Aval, 65p.

Grasso, F., Bismuth, E., Verney, R., 2021. Unraveling the impacts of meteorological and anthropogenic changes on sediment fluxes along an estuary-sea continuum. Sci. rep., 11(1), 1-11. https://doi.org/10.1038/s41598-021-99502-7.

Hobday, A. J., Alexander, L. V., Perkins, S. E., Smale, D. A., Straub, S. C., Oliver, E. C. J., Benthuysen, J. A., Burrows, M. T., Donat, M. G., Feng, M., Holbrook, N. J., Moore, P. J., Scannell, H. A., Sen Gupta, A., Wernberg, T., 2016. A hierarchical approach to defining marine heatwaves. Prog. Oceanogr., 141, 227–238. https://doi.org/10.1016/j.pocean.2015.12.014

Ibrahim, O., Mohamed, B., Nagy, H., 2021. Spatial variability and trends of marine heat waves in the eastern mediterranean sea over 39 years. Journal of Marine Science and Engineering, 9(6), 643. https://doi.org/10.3390/jmse9060643.

IPCC, Masson-Delmotte, V., Zhai, P., Pirani, A., Connors, S. L., Peìan, C., Berger, S., Caud, N., Chen, Y., Goldfarb, L., Gomis, M. I., Huang, M., Leitzell, K., Lonnoy, E., Matthews, J. B. R., Maycock, T. K., Waterfield, T., Yelekçi, O., Yu, R., Zhou, B., 2021. Climate change 2021: the physical science basis. Contribution of working group I to the sixth assessment report of the intergovernmental panel on climate change, Cambridge University Press, 2, 2391 pp.

IPCC, Lee, H., Calvin, K., Dasgupta, D., Krinner, G., Mukherji, A., Thorne, P., ... & Park, Y., 2023: Climate Change 2023: Synthesis Report, Summary for Policymakers. Contribution of Working Groups I, II and III to the Sixth Assessment Report of the Intergovernmental Panel on Climate Change [Core Writing Team, H. Lee and J. Romero (eds.)]. IPCC, Geneva, Switzerland, 42pp.

Izquierdo, P., Rico, J. M., Taboada, F. G., González-Gil, R., Arrontes, J., 2022. Characterization of marine heatwaves in the Cantabrian Sea, SW Bay of Biscay. Estuar. Coast. Shelf Sci., 274. https://doi.org/10.1016/j.ecss.2022.107923.

Jalón-Rojas, I., Castelle, B., 2021. Climate control of multidecadal variability in river discharge and precipitation in western Europe. Water, 13(3), 257. https://doi.org/10.3390/w13030257.

Karl, D.M., Lukas, R., 1996. The Hawaii Ocean Time-series (HOT) program: Background, rationale and field implementation. Deep Sea Research Part II: Topical Studies in Oceanography, 43(2-3), 129-156.

Lamarque, B., Deflandre, B., Schmidt, S., Bernard, G., Dubosq, N., Diaz, M., Lavesque, N., Garabetian, F., Grasso, F., Sottolichio, A., Rigaud, S., Romero-Ramirez, A., Cordier, M.-A., Poirier, D., Danilo, M., Grémare, A., 2022. Spatiotemporal dynamics of surface sediment characteristics and benthic macrofauna compositions in a temperate high-energy River-dominated Ocean Margin. Cont. Shelf Res., 247, 104833. https://doi.org/10.1016/j.csr.2022.104833.

Landemaine, V., 2016. Érosion des sols et transferts sédimentaires sur les bassins versants de l'Ouest du Bassin de Paris: analyse, quantification et modélisation à l'échelle pluriannuelle. University of Rouen. https://hal-normandie-univ.archives-ouvertes.fr/tel-01937208 S.

Lazure, P., Dumas, F., 2008. An external–internal mode coupling for a 3D hydrodynamical model for applications at regional scale (MARS). Adv. water resour., 31(2), 233-250. https//doi.org/10.1016/j.advwatres.2007.06.010.

Le Hir, P., Ficht, A., Jacinto, R. S., Lesueur, P., Dupont, J. P., Lafite, R., Brenon, I., Thouvenin, B., Cugier, P., 2001. Fine sediment transport and accumulations at the mouth of the Seine estuary (France). Estuaries, 24(6), 950-963.

Le Hir, P., Cayocca, F., Waeles, B., 2011. Dynamics of sand and mud mixtures: A multiprocess-based modelling strategy. Cont. Shelf Res., 31(10), S135-S149. http://dx.doi.org/10.1016/j.csr.2010.12.009.

Lesourd, S., Lesueur, P., Brun-Cottan, J. C., Garnaud, S., Poupinet, N., 2003. Seasonal variations in the characteristics of superficial sediments in a macrotidal estuary (the Seine inlet,

France). Estuar., Coast. Shelf Sci., 58(1), 3-16. https://doi.org/10.1016/S0272-7714(02)00340-2.

Lettmann, K.A., Wolff, J.O., Badewien, T.H., 2009. Modeling the impact of wind and waves on suspended particulate matter fluxes in the East Frisian Wadden Sea (southern North Sea). Ocean Dyn. 59, 239–262. https://doi.org/10.1007/s10236-009-0194-5.

McPhillips, L. E., Chang, H., Chester, M. V., Depietri, Y., Friedman, E., Grimm, N. B., Kominoski, J.S., McPhearson, T., Mendez-Lazaro, P., Rosi, E.J., Shafiei Shiva, J., 2018. Defining extreme events: A cross-disciplinary review. Earth's Future, 6(3), 441-455. https://doi.org/10.1002/2017EF000686.

Mengual, B., Hir, P. Le, Cayocca, F., Garlan, T., 2017. Modelling fine sediment dynamics: Towards a common erosion law for fine sand, mud and mixtures. Water, 9(8). https://doi.org/10.3390/w9080564.

Nowacki, D. J., Ganju, N. K., 2018. Storm impacts on hydrodynamics and suspended-sediment fluxes in a microtidal back-barrier estuary. Marine Geology, 404(April), 1–14. https://doi.org/10.1016/j.margeo.2018.06.016.

Oliver, E. C. J., Donat, M. G., Burrows, M. T., Moore, P. J., Smale, D. A., Alexander, L. V., Benthuysen, J. A., Feng, M., Sen Gupta, A., Hobday, A. J., Holbrook, N. J., Perkins-Kirkpatrick, S. E., Scannell, H. A., Straub, S. C., Wernberg, T., 2018. Longer and more frequent marine heatwaves over the past century. Nature Communications, 9(1), 1–12. https://doi.org/10.1038/s41467-018-03732-9.

Poppeschi, C., Charria, G., Goberville, E., Rimmelin-Maury, P., Barrier, N., Petton, S., Unterberger, M., Grossteffan, E., Repecaud, M., Quemener, L., Theetten, S., Le Roux, J.-F., Tréguer, P., 2021. Unraveling salinity extreme events in coastal environments: a winter focus on the Bay of Brest. Front. Mar. Sci., 966. https://doi.org/10.3389/fmars.2021.705403.

Poppeschi, C., Charria, G., Daniel, A., Verney, R., Rimmelin-Maury, P., Retho, M., Goberville, E., Grossteffan, E., Plus, M., 2022. Interannual variability of the initiation of the phytoplankton growing period in two French coastal ecosystems. *Biogeosciences*, *19*(24), 5667-5687. https://doi.org/10.5194/bg-19-5667-2022.

Répécaud, M., Quemener, L., Charria, G., Pairaud, I., Rimmelin, P., Claquin, P., Jacqueline, F., Lefebvre, A., Facq, J.V., Retho, M., Verney, R., 2019. National observation infrastructure: an example of a fixed-plateforms network along the French Coast: COAST HF. Oceans, 1-6. https://doi.org/ 10.1109/OCEANSE.2019.8867451.

Roland, A., Ardhuin, F., 2014. On the developments of spectral wave models: numerics and parameterizations for the coastal ocean. Ocean Dyn., 64(6), 833-846. https://doi.org/10.1007/s10236-014-0711-z.

Salomon, J.-C., Breton, M., 1991. Courants résiduels de marée dans la Manche. Oceanologica Acta, Special issue. 11, 47-53.

Schallenberg, M., Burns, C., 2004. Effects of sediment resuspension on phytoplankton production: teasing apart the influences of light, nutrients and algal entrainment. Freshwater Biology, 49(2), 143-159. https://doi.org/10.1046/j.1365-2426.2003.01172.x

Schlegel, R., Oliver, E., Hobday, A., Smit, A., 2019. Detecting marine heatwaves with sub-optimal data. Frontiers in Marine Science, 6(737). https://doi.org/10.3389/fmars.2019.00737

Schulz, E., Grasso, F., Le Hir, P., Verney, R., Thouvenin, B., 2018. Suspended sediment dynamics in the macrotidal Seine Estuary (France): 2. Numerical modeling of sediment fluxes and budgets under typical hydrological and meteorological conditions. J. Geophys. Res. Oceans, 123(1), 578-600. https://doi.org/10.1002/2017JC013185.

Simon, A., Poppeschi, C., Plecha, S., Charria, G., Russo, A., 2023. Coastal and regional marine heatwaves and cold-spells in the Northeast Atlantic. *EGUsphere*, *2023*, 1-25.

Soulsby, R. L., Hamm, L., Klopman, G., Myrhaug, D., Simons, R.R., Thomas, G.P., 1993. Wave-current interaction within and outside the bottom boundary layer. Coastal engineering, 21(1-3), 41-69.

Stephenson, D., 2008. Definition, diagnosis, and origin of extreme weather and climate events. Clim. extremes soc., 340, 11-23.

Tang, J., Wang, Y. P., Zhu, Q., Jia, J., Xiong, J., Cheng, P., ... & Wu, H., 2019. Winter storms induced high suspended sediment concentration along the north offshore seabed of the Changjiang estuary. *Estuarine, Coastal and Shelf Science*, *228*, 106351. https://doi.org/10.1016/j.ecss.2019.106351.

Tavora, J., Salama, M., Penning de Vries, M., Mannaerts, C. M., van der Wal, D., 2023. Detecting the Effects of Extreme Events on Estuarine Suspended Particulate Matter Using

Satellite Remote Sensing (Scheldt Estuary): Challenges and Opportunities. Remote Sens., 15(3), 670. https://doi.org/10.3390/rs15030670.

Verney, R., Le Berre, D., Repecaud, M., Bocher, A., Poppeschi, C., Grasso, F., 2024. Suspended particulate matter dynamics at the interface between an estuary and its adjacent coastal sea: unravelling the impact of tides, waves and river discharge from 2015-2022 *in situ* high-frequency observations. Marine Geology.

Warner, J.C., Butman, B., Soupy Dalyander, P., 2008. Storm-driven sediment transport in Massachusetts bay. Cont. Shelf Res., 28, 257-282. https://doi.org/10.1016/j.csr.2007.08.008.

Appendix

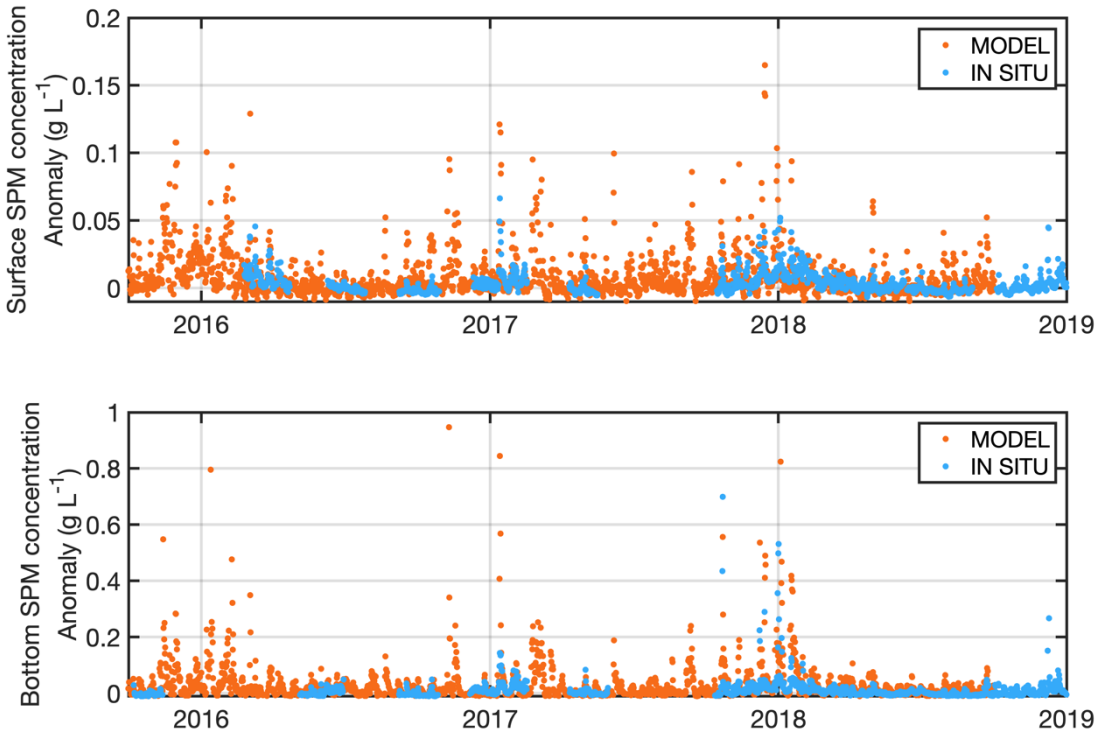

Figure S1. Validation of model SPMC anomaly against surface and bottom *in situ* observations from the SCENES buoy

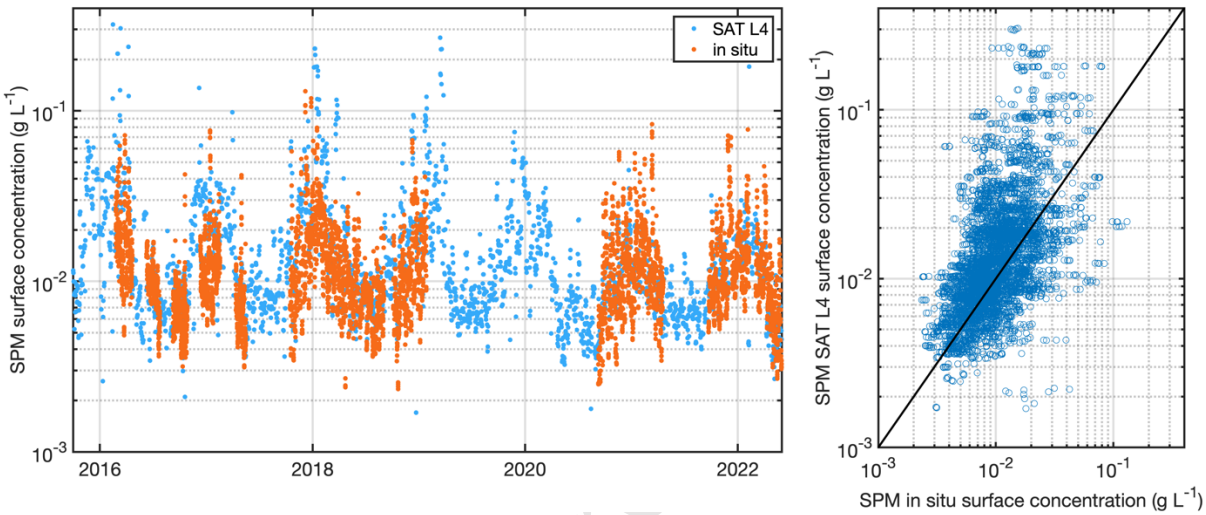

Figure S2. Validation of SPMC (g L^{-1}) data from L4 satellite products against surface observations from the SCENES buoy

Declaration of interests

☒The authors declare that they have no known competing financial interests or personal relationships that could have appeared to influence the work reported in this paper.

☐The authors declare the following financial interests/personal relationships which may be considered as potential competing interests:

Highlights

- Time dependent climatologies were calculated to identify and characterize extreme events from forcings and SPM concentration anomaly datasets
- Extreme event impact is seasonally variable, but relatively as much important in summer as in winter.
- Extreme river flow event become more frequent over the last 60years, but also their seasonality changed, with more intense events reported in April (1892-2001) and May/June (2002-2021), which are usually periods of low river flow.